Table of Contents

1 Table of Figures

3

2 Table of Tables

3 Table of Equations

4 Notes on Structure

The traditional thesis structure is broadly defined as:

- Introduction;
  - Background;
  - Scope; and,
  - Outline.
- Theory;
- Methods;
- Analysis;
- Discussion; and,
- Conclusions.

Due to the nature of the works competed in this thesis liberties were be taken to improve flow, clarity, and communication in general.

As per conventional structures, the project is introduced, and some background information relating to the context of the project is presented. From this the scope and focus of the thesis is derived and defined. Next the project is broken down functionally into the major subsystems required for a successful project (as defined in the scope).

Within each of these subsections standard structure is employed. The purpose and context of the subsystem is explained, and the requirements for practical completion are detailed. Then a literature review is conducted as appropriate for each subsystem, explaining technologies or theory as needed. From this the specific methods, in design and implementation are detailed for each subsystem, e.g. the engineered design, and then the specific technology employed to implement the design. Finally, analysis is conducted based on the outcomes of the subsystem.

The intention of this method is to allow for a consistent singular train of thought, where information on a system is presented sequentially, rather than all information relevant to the thesis presented in order of type.

Once the subsystems are discussed, the same process (scope, requirements, theory, method, and analysis) is applied to the task of integrated all the major subsystems into a single supersystem. This section details the complete system and the performance of the exoskeleton developed. This section presumes knowledge of the subsystems but does not demand knowledge of their intricacies. The intention is that by compartmentalising the details of the subsystems it is possible to discuss the design of the exoskeleton in general with brevity and clarity.

Finally, the results of the project are discussed, before the implications, recommendations, and conclusions of the project are discussed.

Readers primarily concerned with the outcomes of the proof of concept and thesis and not the specifics of how it was done, may find that reading **Error! Reference source not found.** and then skipping to **Error! Reference source not found.** (referencing the earlier sections of the documents as needed) is the most palatable method of consuming the document. Through this they may understand the projects context, what was done, and the results, without the dry technical details.

5 Introduction and Outline

A powered exoskeleton, or exoskeleton, is wearable technology the amplifies and augments the pilot's physicality. Through direct mechanical assistance via actuators, the pilot's effective strength may be increased. By supplementing the strength required to complete a task the energy requirements of the task may be reduced; effectively increasing the pilot's endurance. Possible uses for exoskeletons include: military operations, emergency & rescue, physical/manual labour, and medical applications.

Two major factors impact the viability of exoskeleton technology: power supply, and control. This thesis shall address one facet of the difficulties of exoskeleton control. Current exoskeleton control methods are inadequate due to mechanical constraints and the limitations of the control methods. Imperfections in mechanical design may result in a limited range of movement affecting the suits utility (e.g. A rigid spine in a confined space). Current methods of control use either force-based sensors or preprogramed movements. Finite sets of preprogramed movements are insufficient for dynamic environments (Charara, 2015). Force based methods encounter stability problems and may increase the exertion required to complete a task (Keller, 2016).

Instead this thesis will focus on the development of a novel power exoskeleton control method based on detecting the pilot's position relative to the suit to maintain a constant offset; specifically focusing on the development of the controls and perception systems required to direct an exoskeleton.

An proximity-base control system, by maintaining a constant offset from the user, may exist as a concentric outline (or *bubble*) of the user, mirroring their actions. Thus, to control the system the pilot simply needs to assume the desired position of the suit, and the suit shall mimic them. By mimicking the user's actions, the suit is more intuitive that force based and preprogramed methods. With no physical contact required to operate the system, the energy required from a pilot to complete a task with a load is effectively the same as completing the task with no load. Therefore, with any arbitrary load the user has the endurance to perform the task as if there no load at all.

Kt

5.1 Aim of Thesis

5.2 Summary of Achievements

6 Background and Problem breakdown

6.1 Prior Art

Exoskeleton technology began in 1890 (United States of America Patent No. 440684, 1890), with Nicholas Yagin's development of a passive device that used compressed gas to assist in human movement, see Figure 1.
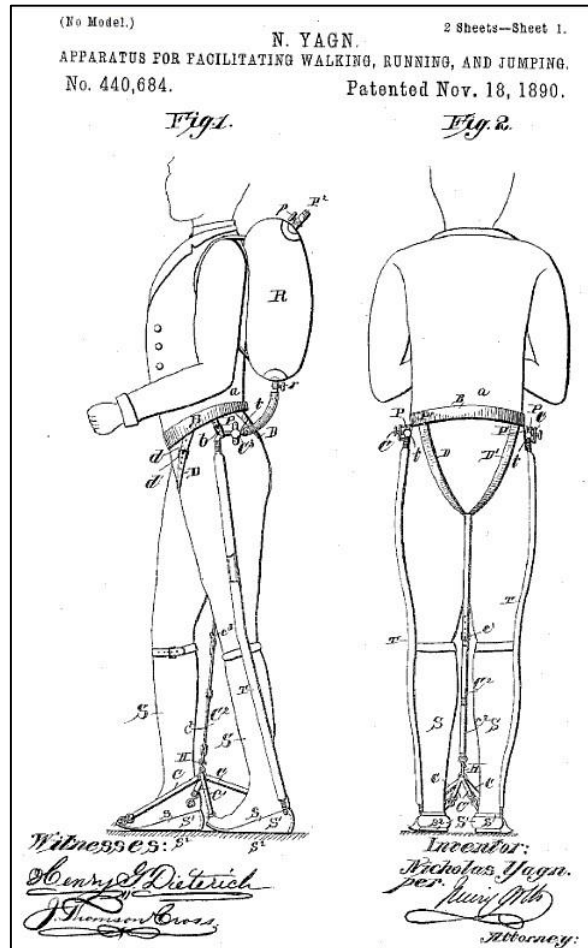
Figure 1: Assisted-walking Device (Cybernetic Zoo, 2010)

However, it was not until the 1960s that the first attempt at a practical powered exoskeleton was developed. The Hardiman (Keller, 2016) shown in Figure 2,created by General Electric, was ground-breaking but non-viable due to its extreme weight (double its maximum load) and control problems. The suit, when used as a complete system instead of in parts, was subject to dangerous violent uncontrolled movements and the master-slave control system suffered debilitating lag.
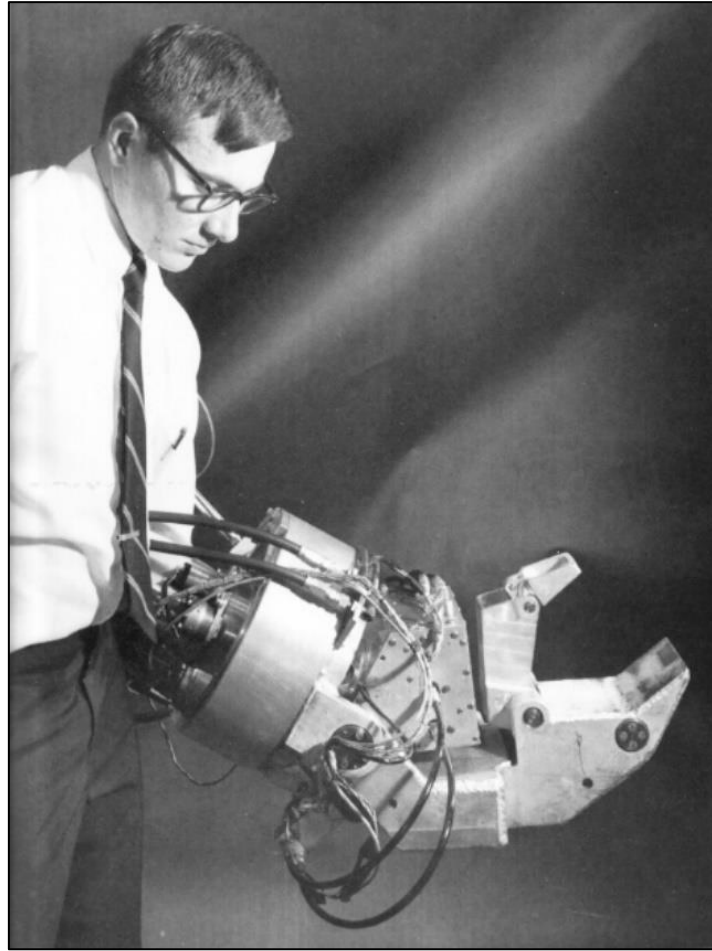
Figure 2: G.E. Hardiman I Exoskeleton (Cybernetic Zoo, 2010)

Prospective uses for exoskeletons usually involve a scenario where a human user may require the strength and endurance of a machine but wheeled vehicles are undesirable. Examples of possible applications include:

- Military Operations: operators are required to carry head loads over longs distances, lift large weights, and operate in dynamic and unruly conditions. Difficult terrain, heterodox environments, and general disarray result in heavy machinery often being unsuitable for certain circumstances. From urban to jungle operation exoskeletons provide possible utility.
- Rescue and evacuation missions: Rescue operations feature similar constraints to military operation with the additional concern of environmental hazards and structural collapse. In the event of a fire or chemical incident, the safety equipment and tools required can be large, heavy, and cumbersome; exoskeletons can alleviate some of this burden. Where structures are damaged or collapsed an exoskeleton can provide the extra strength required to save a life,
- Medical Systems: When amputation, age, or illness results in an individual suffering from reduced mobility and strength exoskeletons present exciting opportunities to compensate for their pilot's impediments.

- Construction & Physical Labour: kt

These applications represent some of the broader uses for exoskeletons, neglecting the role of specifically designed exoskeletons for niche tasks: shock absorbing legs for parachutes/paratroopers, self-propelled underwater diving suits, etc.

Since the Hardiman, exoskeletons have been plagued by the same two major problems that have prevented their use in real world applications: power to weight ratio/power supply and control. The following outlines current developments in exoskeleton technologies.

6.1.1 HULC

The Human Universal Load Carrier (HULC) is battery-powered lower extremity exoskeleton initially developed by Berkeley Robotics and Human Engineering Laboratory, before entering an exclusive licensing agreement with Lockheed Martin in 2009 (Axe, 2012). The system uses hydraulics to amplify the pilot's knees and hips while supporting a load of up to 90kg. Designed for military applications it claims six hours of battery and uses force-based sensors for control.

The HULC was abandoned as" it proved impractical, exhausting users instead of supercharging them" (Cornwall, 2015) and has been succeeded by the TALOS project (Cornwall, 2015).

6.1.2 EskoGT

In 2010 the original developer of the HULC, Esko Bionics revealed the Exoskeleton Lower Extremity Gait System (eLEGS) (Charara, 2015). With a maximum battery life of 6 hours and maximum gait of 3.2m/s (Charara, 2015), the system uses pushbuttons and force-motion sensors for control. Specially design for medical applications, the exoskeleton uses preprogramed movements to aid the mobility of stroke and spinal injury patients.

The suit is ill suited for dynamic environments as its finite range of movements prohibits uneven surfaces. While the suit may assist those with "upper extremity motor function of at least 4/5 in at least one arm" (Charara, 2015), the suit is slower than a wheelchair and is not an improvement on standard human movement.

6.1.3 Raytheon XOS Exoskeleton

The 2008 Raytheon XOS Exoskeleton developed by Raytheon is a full body exoskeleton that can support up to 23kg on each arm (Karlin, 2011). The suit uses force-based sensors for control. Despite claims that the exoskeleton would be ready for production by 2016, they have made no public comments on progress since 2011 (Karlin, 2011).

6.1.4 Warrior Web

The Warrior Web non-rigid exoskeleton was first demonstrated at the 2016 DARPA Demo Day (Cornwall, 2015). Developed by DARPA, it used preprogramed

commands to assist with the user's ankle motions. However, it was unpredictable in uneven terrain, malfunctioned, and could not transition readily between a walking and running state (Cornwall, 2015).

6.1.5 Hybrid Assistive Limb (HAL)

In 1997 Cyberdyne unveiled the Hybrid Assistive Limb (HAL) (Cyberdyne, 2016). The HAL's iterations include a battery-powered lower extremity exoskeleton and a full body exoskeleton (Cyberdyne, 2016). Through a combination of bioelectrical sensors and force sensors the HAL measured muscle contracts to trigger preprogramed movements.

The system has had mixed success, and despite applying for USA FDA approval in 2014, the HAL is yet to be permitted for use in the US (Cyberdyne, 2015).

6.1.6 Preprogramed Control

Preprogramed control methods consist of a set of specific movements that are triggered in one way or another. HAL measures contractions in the arms of patients to trigger left-foot right-foot walking motions. Warrior Web applies torque to the ankle of the user (assisting them walk) when movement is detected.

These systems are inherently limited in their utility. By having a finite or procedurally generated set of movements there will always be scenarios or circumstances where the set of movements is not applicable. In real dynamic environments (e.g. military, rescue & evacuation, and physical labour) dynamic controls are required.

As noted by Dunietz when using an exoskeleton with preprogramed controls, the "human does try to join in the motion, the two get in each other's way, cancelling out the gains for all but the most extreme disabilities." (Dunietz, 2017). Through this we seem the limited applicability of preprogramed movements; in circumstances where the movement of the pilot is so limited and restricted (e.g. via disability) that any system is an improvement. For an able-bodied pilot preprogramed movements are "a bit like being a marionette with four wires controlling my legs" (Cornwall, 2015) and inadequate.

6.1.7 Force Based Control

Force based control systems use force applied to the internals of a suit to determine the users desired position. The force applied indicates the direction and magnitude of movement. Force based systems are often inadequate for practical applications due to the sensitivity of force input. Systems which are too sensitive may develop jitter, and delays between sensing and movement combines with physical inertia may result in the system applying force to the user, creating an unstable feedback loop. Systems with are insensitive are slugging and require the pilot to push and move against the suit. Using these systems can be cumbersome and exhausting to use.

As the only mechanism for detecting position for a force-based system is the user making contact with the suit, misalignments in sizing can result physical dead bands when users are unable to touch the suit and the control system is effectively blind. Additionally, suits which maintain constant contact with asymmetrical body parts may interpret asymmetry as force input and therefore require constant active resistance from the user to control.

Finally, force-based systems do not distinguish between the force output of the system and the speed desired. If a user wishes to move quickly they must apply a large amount force to the system, if the suit encounters an obstacle this movement is then interpreted as a large amount of force applied to the object. There is no mechanism for quick safe movements.

For exoskeletons in dynamic real-world environments to be viable improvements on the existing force-based sensing methods are required.

6.2 Proximity as a solution

Consider the following:

a) For controlling the suit, it may be assumed that the user is inside the suit during operation;
b) The users desired position for the suit may be treated as their position;
c) Thus, the positional error between the desired configuration of the suit and the actual configuration of the suit is the difference between the configuration of the pilot and the configuration of the exoskeleton;
d) If the position of the pilot relative to the suit is measured and known, then the position of the suit relative to the pilot can be known; and,
e) Therefore, the suit can be controlled accurately (that is to say, error can be known at any time) by observing the position of the pilot relative to the suit

It is proposed to develop a proof of concept for an positional exoskeleton control system based on measurement of the pilot's position/proximity the suit. By maintaining a constant offset from the user, the exoskeleton may exist as a concentric outline (or *bubble*) of the user, mirroring their actions.

Consider the following:

a) In a circumstance where the exoskeleton encounters an obstacle it is desirable to regulate and control the force output of the system;
b) It is desirable to decouple the control of force output and speed (a noted flaw with force-based control methods);
c) To ensure safe movement that does not apply undue force to the environment, the force output of the exoskeleton should be measured and regulated at external contact points.

It is proposed that for the exoskeleton that the force output is directly measured (at contact points) to ensure safe and controlled operation.

Consider the following:

a) If the system applies force up to a safe maximum, then once that maximum is met then the exoskeleton will stop matching pace with the user's movement;

b) Under these circumstances the constant offset between the user and the system will not be maintained;

c) The user then may make contact with the internals of the exoskeleton;

d) It is possible to use the pilot's continuing attempts to towards the obstacle as intent to increase force output of the suit;

e) By measuring the force applied by the user to the inside of the exoskeleton at contact points it may be possible for the user to indicate the desire for increased force output;

f) By measuring the force applied to external and internal contact points by the exoskeleton and the pilot respectively it is possible for the exoskeleton to operate with safe low force outputs which a pilot may override when increased force output is desired; and,

g) By using this system when the actuators are capable of strength beyond normal human capabilities, the pilot can effectively command and control superhuman strength in a safe and intuitive manner.

To properly control the force output of the system the forces applied internally and externally to the exoskeleton shall be measured, and the force applied by the user to the internals of the exoskeleton shall be used to control the force output of the systems actuators.

The subsequent system in summary:

- Uses position sensors to determine the desired configuration of the exoskeleton from the bodily configuration of the pilot;
- Uses external sensors to regulate the force output of the system, maintaining a safe maximum; and,
- Measures force applied internally to determine the force output of the system.

The potential benefits of such a system are summarised as follows.

6.2.1.1.1 Dynamic control

By mirror the movements of the user, with a sufficient mechanical design, the system is only limited by the capabilities of the pilot. Therefore, in any system which a human could navigate the system should be able to operate. Compared to preprogramed systems, it will be possible to navigate uneven terrain, switch contexts, and perform in unpredictable environments.

6.2.1.1.2 Intuitive control

The system described shall provide more intuitive control relative to other solutions. If the pilot seeks to move the left leg of the system, they must simply move their left leg. If the suit makes contact with an object the exoskeleton will cease movement. If the pilot wishes to push the object, they simply need to push the object through the suit. The pilot may control the exoskeleton as they would their own body.

6.2.1.2 Effortless operation

The system significantly increases the effective endurance of the pilot while requiring no exertion to use. Using the example of carrying a heavy load; for the user to walk normally requires a set amount of effort. With no load applied to the exoskeleton the action should require the same amount of effort. With a sufficiently strong exoskeleton, the system may be loaded with any arbitrary weight, but the effort required by th user to walk will remain unchanged. The exoskeleton effectively gives the operator carrying a load the endurance of an operator with no load. Note, the magnitude of this benefit increases as the load increases.

6.2.2 Functionality Requirements

To determine the viability of the exoskeleton and develop a proof of concept it is essential to define the required capabilities of such a system. The following outlines the requirements for a functional exoskeleton system:

1. The system must be capable of steady-state/static operation;
2. The system must be capable of dynamic and actuated operation;
3. The system must be capable of dynamic and actuated operation with non-regulated/imprecise force application;
4. The system must be capable of dynamic and actuated operation with regulated force application; and,
5. The system must be capable of dynamic and actuated operation with regulated force application under real-time conditions.

Should the system be capable of achieving level 5 operation it can be said to be fully functional. To assess the system's level of functionality specific test case are required which may be considered representative movements of the requirements of each level of functionality. These are outlined as follows in Table 1.

Table 1: Functional levels and associated movements

Functionality Level	Representative Movement	Position of Pilot	Position of Exoskeleton	Force Applied by Pilot	Force Applied by Exoskeleton
L1	Standing	✓	✓		
L2	Squatting	✓	✓		
L3	Stairs	✓	✓		

| L4 | Sitting | ✓ | ✓ | ✓ | ✓ |
| L5 | Sprinting | ✓ | ✓ | ✓ | ✓ |

As seen in Table 1, there are four main pieces of information required to control the exoskeleton at all levels. From the required information it is possible to create a system that can demonstrate all levels of functionality. Note that every representative movement can be completed using only the lower extremities. This implies that to develop a proof of concept for exoskeleton only a lower extremity exoskeleton would be required.

6.3   Controls

> "A control system is an interconnection of components forming a system configuration that will provide a desired system response."
> *(Ogata, 2010).*

A closed loop control system uses feedback and measurements to compare the system with the desired output. By modelling a system and developing the appropriate controls system we may generate the desired behaviour from the system.

A closed loop control system, see Figure 3, can be summarised as the interaction of (Ogata, 2010):

- Controllers: which are informed of the desired behaviour while receiving feedback from sensors on the actual behaviour of the system;
- Actuators: which modulate their behaviour based on instructions from the controllers;
- A process to be controlled; and,
- Sensors: which measure the behaviour of the system (the actual output of the process) and inform the controllers.
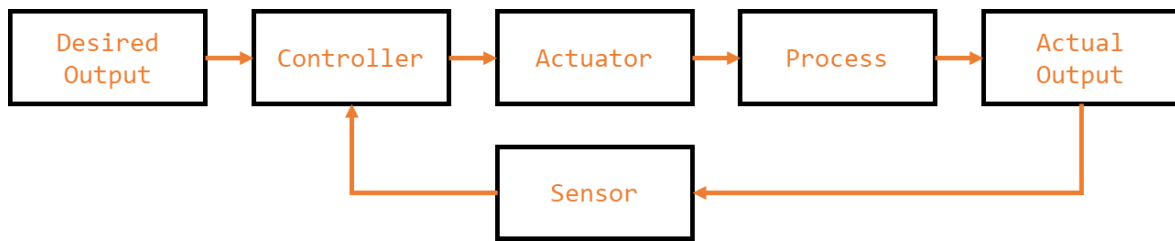
Figure 3: Closed Loop Control System

One method of conceptualizing the behaviour of a system is to create block diagrams of the system (Golnaraghi & Kuo, 2010). Block diagrams may be used to communicate comparators, transfer function components, input and output signal, feedback loops, etc. We may describe the state of a closed loop system via block diagrams, see Figure 4.
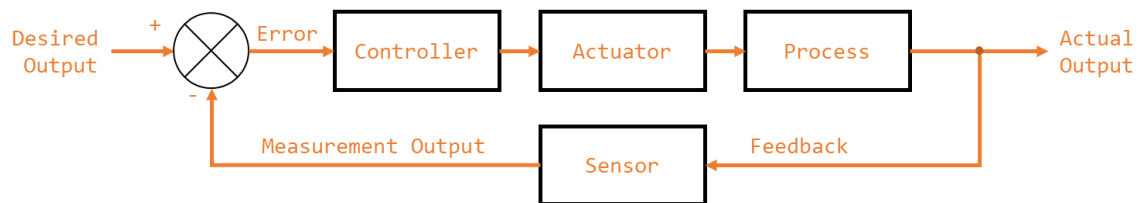
Figure 4: Closed Loop Control System Block Diagram

Here the error of the system is the difference between the desired state and the measured state. The (usual) goal of controls is to reduce the error to zero. This may

be accomplished by numerous methods, which include the transfer function method[1].

6.3.1 Transfer Function Approach to Modelling and Control

> *"The transfer function of a linear, time-invariant differential-equation system is defined as the ratio of the Laplace transform of the output (response function) to the Laplace transform of the input (driving function) under the assumption that all initial conditions are zero."* (Otaga, 2004)

We may define the transfer function, $G(s)$ for a system as given by Equation 1; where $X(s)$ is the Laplace transform of the input and $Y(s)$ is the laplace transform of the output. This may be seen diagrammatically in Figure 5. The transfer function allows us to map from a set of inputs to the outputs of system.

$$G(s) = \frac{X(s)}{Y(s)}$$

Equation 1: Transfer Function

Figure 5: Transfer Function

For a closed loop system, we may say that the behaviour of the system, as seen in Figure 6, may be described by the relationship of the control system and the system process with respect to the error (Golnaraghi & Kuo, 2010).
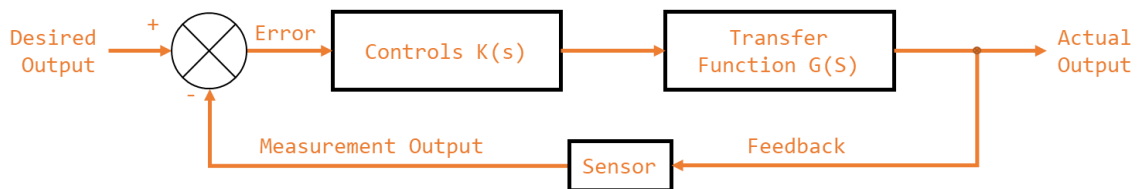
Figure 6: Controlled Closed Loop System

We may minimise the error of the system by correctly curating the control system (K). This is to say, given a system described by G(s), by controlling K(s) (the controllers and actuators) we can ensure that the actual output of the system is the desired output of the system (Otaga, 2004). The transfer function for this system, based on the block diagram in Figure 7, is given by Equation 2.

---

[1] The root locus method could be used to develop the controls for the system. However, that would just be a recount of Ogata and as such we refer to Modern Control Engineering (Ogata, 2010), rather than repeating it. Chapter 6 addresses design by the Root-Locus Method and Chapter 10 speaks directly regarding servo system design (a perhaps more apt framing of the 'actuators side' of the project).

Figure 7: Controlled Closed Loop System (Parameterised)

$$H(s) = K(s)G(s)$$

$$C(s) = E(s)H(s)$$

$$E(s) = R(s) - B(s) = R(s) - C(s)$$

$$C(s) = H(s)\big(R(s) - C(s)\big)$$

$$TF = \frac{C(s)}{R(s)} = \frac{H(s)}{1 + H(s)}$$

Equation 2: Controlled Closed Loop Control System Transfer Function

6.3.2 Proportional–Integral–Derivative controller

A proportional–integral–derivative controller (PID) is a method of developing the controls parameters (and K(s)) for a system.

One approach to controls is to amplify the actuators response proportionally to the error. This is known as proportional control and is shown in Figure 8.
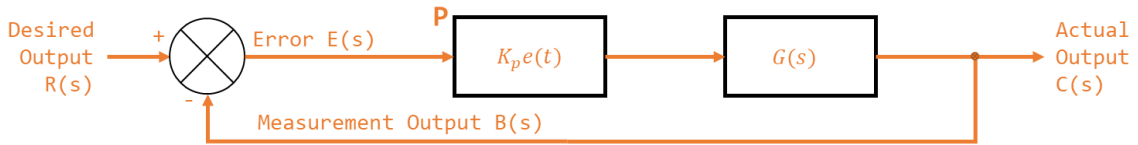
Figure 8: P Control

If the proportional gain of a system is too small the response time of the system may be too slow. If the value is to high the system may overcompensate, resulting in oscillations and overshooting of the target values. If the proportional gain is sufficiently high the system may oscillate so wildly that it becomes unstable (Otaga, 2004). Unstable meaning the system never reaches the desired output and the error of the system increases over time. (National Instruments, 2018).

Proportional control is effective at addressing the gross present error in the system. To create a fast response time for a system, without increasing the proportional gain to unstable values often a derivative term is employed.

Figure 9: PD Control depicts a system with a proportional (K_p) and a derivative gain (K_d). K_d changes in response to the rate at which error is changing. By incorporating a proper K_d value the system can effective pre-empt change in error, leading to a faster response time (Ogata, 2010).
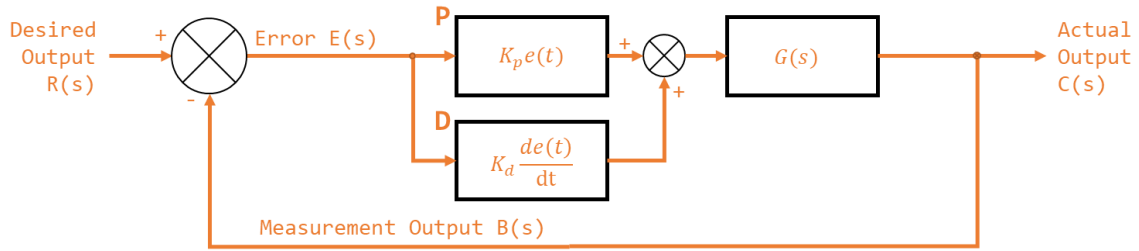
Figure 9: PD Control

A K_d value that is too low will result in a system that doesn't react strongly to changes in error. A K_d value that is correctly calibrated will result in a system that reacts strongly to sudden changes in the system. A K_d value that is too high will reacts too strongly to changes in error and will become highly sensitive to signal noise. Small changes in absolute error which would be ignored by the proportional term may illicit an unwarranted response from an overly sensitive K_d.

For small errors the proportional gain may be insufficient for correction and increasing the proportional gain may result in instability. For constant small errors the change in error may be too small for the derivative gain to correct and increasing the derivative gain may result in instability. Small persistent error in the system, otherwise known as steady state error, may exist in a system with pure PD control.

To compensate and correct the steady state error in a system an integral gain term may be introduced. A system with an integral gain may be seen in Figure 10. The integral gain in practical terms accumulates historical error in the system. This way, even small errors can slowly increase the integral term to an actionable magnitude.
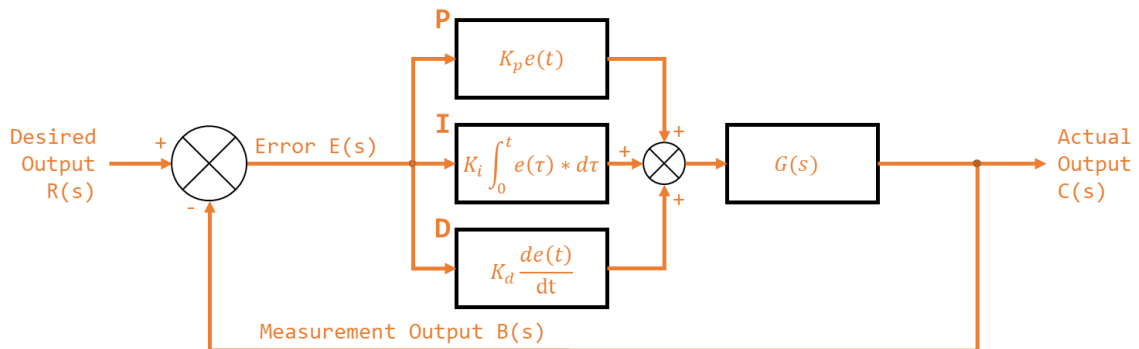
Figure 10: PID Control

An integral gain that is too small will take a very long to correct steady state error within the system. An integral gain that is too large will suffer from integral windup, specifically excessive overshooting the target value. Integral windup is phenomena where a sudden and large change in error cause the integral term to accumulate a massive error that saturates the entire PID response leading to overcompensations. An integral gain that is too large may result in integral wind up of sufficient magnitude that the system becomes unstable.

20

The transfer function for a PID controller is given by Equation 3.

$$K(s) = K_p + K_d s + \frac{K_i}{s}$$

Equation 3: PID Transfer Function

6.4 PID Tuning

There is a plethora of methods for finding the correct range of values for a systems PID to achieve the desired controls, excellent sources include: Automatic Control Systems (Golnaraghi & Kuo, 2010), Modern Control Engineering (Ogata, 2010), Springer Handbook of Robotics (Siciliano & Khatib, 2016), and Modern Control Systems (Dorf & Bishop, 2011). Two were used in this thesis:

- Software tools, specifically MATLAB's PID tuner pidTuner; and,
- The second Ziegler-Nichols method for empirical PID Tuning.

6.4.1 Ziegler-Nichols PID Tuning

The second Ziegler-Nichols (ZN) method entails (Ogata, 2010):

Initialise the K_d and K_i terms to 0 (Equation 4). Note, that in the literature (Ogata, 2010), K_d and K_i are expressed as the T_d and T_i in terms of the K_p (Equation 5) to generate a control transfer function of Equation 6.

$$K_d = 0 \ \& \ K_i = 0$$

Equation 4: ZN Initial Values

$$T_d = \frac{K_d}{K_p} \ \& \ T_i = K_i K_p$$

Equation 5: ZN Convention

$$K_{\text{Ziegler−Nichols}}(s) = K_p \left(1 + T_d s + \frac{1}{T_i s} \right)$$

Equation 6: ZN TF

1. Beginning at 0, increase K_p slowly to the *critical value*, K_{cr}. Where K_{cr} is the lowest K_p "at which the output of the system exhibits sustained oscillation" (Ogata, 2010);
2. Determine the corresponding period (P_{cr}) of K_{cr}; and,
3. Using P_{cr}, K_{cr}, and the values given in kt find the approximate PID values for the system.

Table 2: Ziegler-Nichols Tuning Rules

Controller Type	K_p	T_i	T_d
P	$0.5K_{cr}$	∞	0
PI	$0.45K_{cr}$	$0.833 \cdot P_{cr}$	0
PID	$0.6K_{cr}$	$0.5P_{cr}$	$0.125P_{cr}$

Note that the Ziegler-Nichols parameters attained are not be taken as absolutes. They are systematically determined estimates of the optimal values. Once found empirical testing should be conducted to refine the values and ensure stability.

7 Scope

7.1 Proof of Concept

The purpose of this thesis is to develop some of the major subsystems for a proof concept for a position-based exoskeleton control system. As noted above in 6.2.2, to create a proof of concept for the system only a lower extremity exoskeleton is required.

7.1.1 Task Division

Creating said proof of concept however, is beyond the scale and scope of a single undergraduate thesis. Instead, the task was to be divided amongst two students, who would complete subsystems independently before integrating their work. It was eventually determined that the most elegant and functional demarcation of tasks would be to divide the system according to determining the required actions and performing the required actions. As such one student would be responsible for determining the required action from the exoskeleton systems to perform as desired, and one student would create a system that was capable of performing said actions. Broadly speaking, one student would design and create the sensing/perceiving and control systems for the proof of concept, and the other would create the structural and actuation systems of the proof of concept. The point of integration between the two systems would be a communication system capable of transmitting the desired action from one side to the other.

This student, Samuel Williams, was assigned the perception and control systems.

As a matter of clarification, it is important to note that the terms: actuation system, control system, perception system, and structural system are descriptive terms for the approximate scope and manner of certain groups of subsystems. They are not prescriptive and should not be treated as such, e.g. the mechanical structure required to hold the force sensors in place is structural but is within the scope of the perception systems not the structural system.

7.1.2 Required Systems

A full functional decomposition can be found in 8.

Based on the specific division of tasks and the demarcation devised the following major functional requirements where identified.

1. Detection of Pilots position relative to the exoskeleton (detection of the suit's absolute position would be the responsibility of the actuation system)
2. Force application of the exoskeleton to the environment and the pilot to the exoskeleton
3. Control system for determining required action (torque) from actuation system for correct operation
4. Communication from control & perception software to actuation system

7.1.3   Inclusions (In Scope)

The commissioning of the following was considered within the of scope and the project:

- A lower extremity exoskeleton;
  - This includes feet, shins, thighs, and waist.
- Systems required to perceive the position of an exoskeleton pilot relative to the exoskeleton;
  - This includes the hardware, firmware, software, and mechanical structure required.
  - This is limited to detection of the position of the femur, tibia, and foot (treated as a singular entity). This does not include the detection of the position of individual toes or the internal actuation of the foot.
- Systems required to perceive the force applied by an exoskeleton pilot to an exoskeleton;
  - This includes the hardware, firmware, software, and mechanical structure required.
  - This is limited to the detection of force application at the soles of the feet and the rear of the pilot, zones required for the representative movements.
  - This is limited to a rigid sole without actuation, i.e. the foot may move and bend at the ankle but shall not be treated as flexing at the ball of the foot.
- Systems required to perceive the force applied by exoskeleton its environment;
  - This includes the hardware, firmware, software, and mechanical structure required.
  - This is limited to the detection of force application at the soles of the feet and the rear of the pilot, zones required for the representative movements.
  - This is limited to a rigid sole without actuation, i.e. the foot may move and bend at the ankle but shall not be treated as flexing at the ball of the foot.
- Controls theory required to determine the desired position of the exoskeleton; and,
  - This is limited to determining the desired torque and angle of the actuation systems.
  - This does not include determining power, voltage, or current requirements for actuators.
  - This does not include determining control inputs (e.g. pulse width modulation duty cycles) for the actuation systems.

- Communication systems required to relay system readings and desired actions between actuation system and controls system.
  - This is limited to creating an input and output connection for interfacing with the actuation & structural system via a common protocol.
  - This does not include the implementation of a communication protocol for the student responsible for the actuation & structural systems.

7.1.4 Exclusions (Out of Scope)

The following tasks were considered out of scope and where excluded from the project:

- Commissioning of the torso, head, or upper extremities of an exoskeleton;
- Commissioning of actuation and structural systems required to support and actuate a lower extremity exoskeleton;
- Measurement of actuator positions or absolute exoskeleton position;
- Measurement of velocity, acceleration, or torque of any section of the exoskeleton;
- The development of an exoskeleton capable of supporting additional loads, i.e. carrying weights beyond those required for demonstration of proof of concept;
- There was no compensation for the flexion and distortion of body parts, e.g feet;
- Addressing power consumption problems, power-to-weight ratio problems, or price problems associated with exoskeletons;
- Actuation points (hip, knee, ankle) where constrained to 1 degree of freedom (DOF); and,
- Anything not in scope.

7.2 Variations

The original proposed scope did not include the creation or design of any actuations, or the interfacing between the control and perceptions systems and the systems actuators. As the project progressed it became apparent that the mechanical/actuation section of the project would not be completed in time for proper operation and that to properly develop and demonstrate the functionality of the controls and perception system a testing rig would be required. As such, the original scope of the project was extended to include the design and create of a simplified actuation system capable of refining, testing, tuning, and demonstrating the controls and actuation systems.

Consequentially, a fifth major function requirement was added to the system:

5. Development of actuation system sufficient to demonstrate attainment of other major function requirements.

7.2.1 Inclusions (In Scope)

The following was considered within the of scope and the project:

- Commissioning of actuators and mechanical structure required to demonstrate functionality of position detection systems;
- Commissioning of actuators and mechanical structure required to demonstrate functionality of force detection systems;
- Development of motor interface and power systems required to control actuators in the desired fashion.

No new exclusions were added to the project.

8 Functional Decomposition

The system defined by the scope, see 7, was decomposed into its major function requirements as seen in 7.1.2. Functional decompositions were then completed for the major subsystems in their respective sections (see **4**, **10**, **11**, **12**, and **13**). This section outlines that major function requirements of the system.
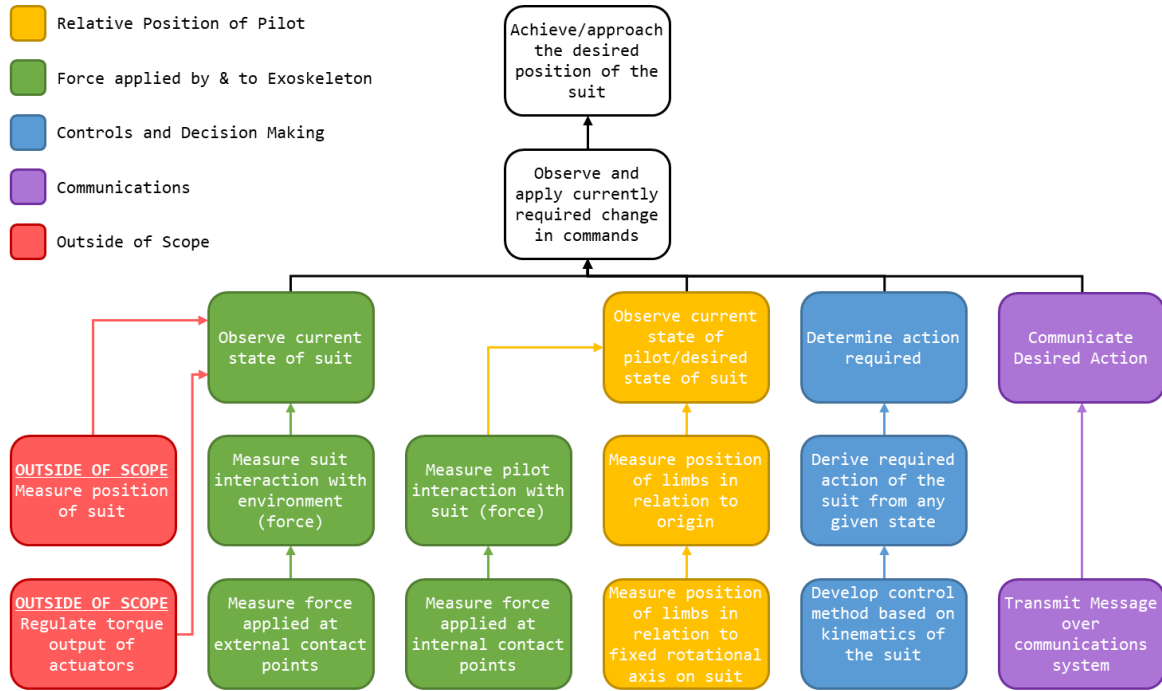
Figure 11; System Decomposition

As seen in Figure 11; System Decomposition, he ultimate goal of the project is that all times the lower extremity exoskeleton will be in the desired position. This may be accomplished by constantly observing the differences between the current state of the system and the desired state of the system and then changing the current system accordingly.

To observe the desired state of the system the position of the pilot and the force applied by the pilot to the exoskeleton must be known.

As seen in Figure 12: Point and Angle to Orientation, the position of a straight linear rod of a fixed length can be described by the relation of a point on the rod (as an angle) to a fixed rotational axis and origin. By observing the angle of a rod relative to an axis we can know the orientation of said rod. Therefore, to determine the current state of the pilot it is possible to observe the location of each limb segment (treated as a straight rod) in relation to a fixed rotation axis.
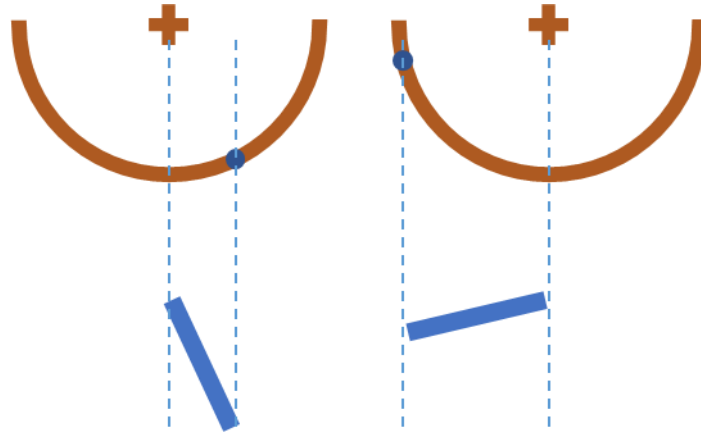
Figure 12: Point and Angle to Orientation

If the rotational axis of the actuation points of the exoskeleton alight with the rotation axis of each limb segment (assuming the hip, knee, and ankle may be treated as 1 DOF hinges) then the position of each limb in relation to the actuation point may be used to determine the position of each limb. By observing the position of the pilot's limbs in relation to the suit, it is possible to know where the pilot is positioned (assuming the position of the suit is known).

As stated in 6.2, the pilot may apply force to the internals of the exoskeleton to indicate the desire to increase the force output of the suit. As a result, the force applied to the internals of the suit must be measured. For the representative motions required for a proof of concept; contact is only required with the ground and a seat, therefore the only locations where force output is required is the rear and the soles of the feet. Only knowledge of the force applied to the internals of the suit at contact points is required to maintain control.

By observing the actual state of the exoskeleton, it is possible to determine the changes required to approach the desired configuration of the exoskeleton. The force/torque output of the actuators of the system is consider out of scope, and the position of the actuators and the absolute position of the suit is considered out of scope. However, the force applied by the system to its environments is within scope and must be determined to identify if force output of the exoskeleton should be changed.

For the representative motions required for a proof of concept; contact is only required with the ground and a seat, therefore the only locations where force output is required is the rear and the soles of the feet. Only knowledge of the force applied to the externals of the suit at contact points is required to maintain control.

In order to determine the action required of the system once the state of the pilot and the state of the exoskeleton are known the kinematics of the suit and the system response in a given state must be known.

To communicate between devices and between the actuation and perception/controls systems it is necessary to transmit messages in a predefined format.

9 Subsystem One: Relative Position of Pilot

This section details the analysis, design, implementation, and results of the subsystem responsible for the perception of the position of the pilot relative to the exoskeleton.

9.1 Definition and Requirement

The overarching purpose of subsystem one (SS1) was to detect the position of the pilot relative to the position of the exoskeleton in real time. This may be accomplished, as noted in **6.2**, by measuring the position of limbs in relation to fixed rotational axis on suit.
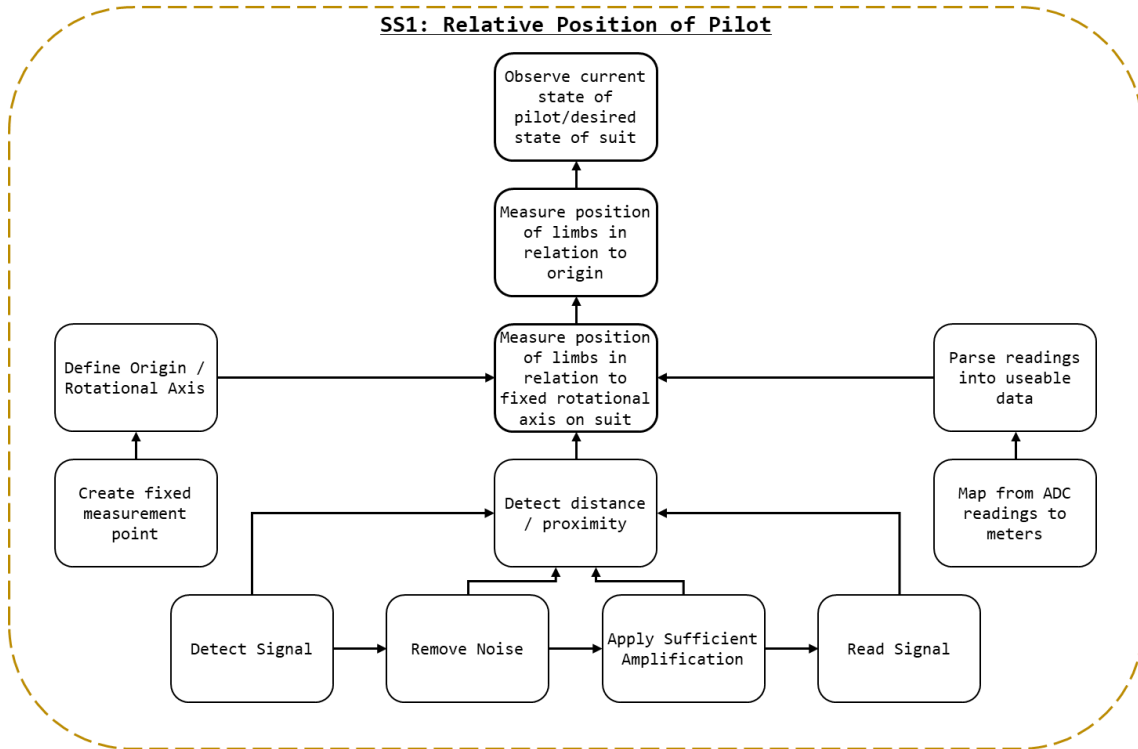
Figure 13: SS1 Breakdown

As detailed in Figure 13: SS1 Breakdown, to measure the position of limbs in relation to fixed rotational axis on suit:

- a fixed rotational axis must be defined;
  - this implies a fixed point where readings can be taken, as such, a mechnism for fastening the detection system must be devised.
- the position/distance must be measured; and,
- the measured distance must be parsed from raw values into useable data.
  - Functionally, this is the process of deriving the function that maps raw analogue voltage values to distance.

The process of measuring the distance will ostensibly entail:

- detecting a signal; the specific type will depend on the techonlogy selected (e.g. IR light, ultrasonic waves, magnetic field strength, etc);
- removing noise from the detected signal; ostensibly through the use of a filter;
- amplifying the cleaned up signal into a range suitble for reading; and,
- reading the signal, ostensibly with an ADC, into a format that can be parsed by the control systems.

9.2 Background and Prior Art

The process of defining the fixed rotational axis and parsing readings into distance values are dictated by the system and are less subject to variation and subjectivity. Instead, the focus on researching prior art for SS1 was determining the most appropriate mechanisms for detecting distance. Additionally, research was conducted on appropriate filtering and amplification methods. The requirements for reading the signals synthesised are outlined, but the selection of a microcontroller for interfacing with all five subsystems is detailed in **Error! Reference source not found.**.

9.2.1 Perceiving Distance

This section details many of the technology considered for perceiving the proximity of the pilot's limbs. The sensor types given the most serious consideration are detailed here, with additional sensors types considered found in 19.3.

9.2.1.1 *IR Transceiver*

Infrared light, or IR, is a form of electromagnetic (EM) radiation general not visible to human eye's (Lynch & Livingston, 2001). The wavelength of IR is typically defined as ranging from 700 nanometres (frequency 430 THz) to 1 millimetre (300 GHz) (Liew, 2018). IR is emitted by the sun, artificial lighting, fires, as thermal radiation from objects (and animals), and from IR emitters (American Technologies Network Corporation, 2018).

The prototypical IR emitter is a light emitting diode (LED) composed to emit IR when power. They typically share a formfactor with standard LEDs and are often used in IR communication. To receive a signal transmitted via an IR emitter and IR received is used. IR receivers may take the form of a photoresistor configured for IR range light. IR emitters and receivers are often used in concert to transmits a message (via the emitter) and then receive it (via the receiver) (Future Electronics, 2018).

Like all EM waves, IR suffers from attenuation (Garbett, 2001). IR is also capable of being reflected off a non-absorbing material. As seen in Figure 14: IR Proximity Sensing, by emitting IR (A) and measuring the intensity of the light reflected (B) it is possible to determine the distance from the reflective surface (C) and the

emitter. This principle may be applied to determine the distance of an object from a transceiver (IR emitter/transmitter and receiver).
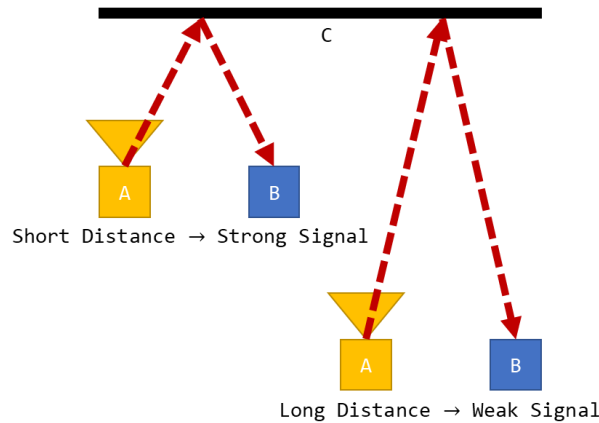
Figure 14: IR Proximity Sensing

IR is an effective method of detecting range, in fact IR is often employed in LiDAR (Cracknell & Hayes, 2007). Assuming line of sight exists between the reflection point and the IR receiver there is no minimum range. Additionally, IR technology is small, affordable, and ubiquitous. Under ideal conditions an IR transceiver would be capable of perceiving the instance between an exoskeleton and its pilot.

Outside of ideal conditions complications with IR technology can occur. As noted above, IR is ubiquitous and is emitted by the sun, artificial lighting, and animals meaning that even if all undesirable frequencies (e.g. the 38kHz carrier signal from most IR remotes) where filtered from an IR signal noise may still exist. Under poor operating conditions an IR transceiver may be saturated with IR rendering it effectively blind. Additionally, variability in the reflective surface may result in IR being reflected inconsistently or not at all. Under these conditions mapping from signal intensity to distance may be impossible, as different surfaces will yield different signal intensities.

9.2.2 Filters and Amplification

This section details the theory required for understanding the requirements and design of the filter and amplifier designed for the proximity perception system.

Filters are applied in order to remove noise from a signal, noise defined as "irrelevant or meaningless data or output occurring along with desired information" (Merriam-Webster Dictionary, 2018). An active filter is a filter that uses active components (e.g. operational amplifiers), rather than entirely passive components. Depending on the nature of the noise present in a measured input specific input ranges may need to be filtered (e.g. unwanted frequencies).

A low pass filter is a filter that permits lower frequency signals and filters high frequency noise, with a high pass performing the opposite function. In the case

where a specific signal frequency is desired a high pass and a low pass filter may be combined to allow a specific band of frequencies to remain. This configuration is known as a band pass filter.

A common and useful electronic filter topology is the Sallen–Key topology. The Sallen–Key topology is an electronic filter topology that allows for the simple implementation for a second order filter. Seen in kt, a band pass filter may by implemented in Sallen–Key topology.
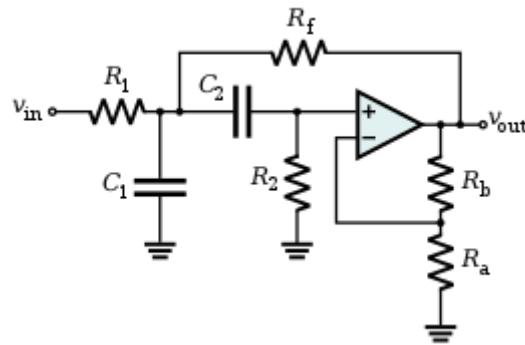
By performing analysis on the circuit depict in figure kt, it is possible to determine the system response of a Sallen–Key bandpass filter.

TALK ABOUT WHAT EQUATIONS WE GET AND HOW THEY CAN BE USED HERE

Kt kt kt

Amplification can be applied to signal to increase its intensity. Within the finite window that is inherent to all measurement mechanisms amplification may be used to increase or decrease the relative signal strength so that the area of interest aligns with the range of measurement. In the context of proximity sensing where the signal intensity may vary (e.g. IR range finding) it may be possible amplify the specific regions on interest. For example, for a signal that ranges between 0-5V for a range of 0-1m being read by and ADC (analogue to digital converter) with a 0-5V range, it may be possible to amplify the signal such that the 10-20cm range constitutes the entire 0-5V range received by the ADC.

9.3 Approach and Execution

9.3.1 Perceiving Distance

When considering the conditions of operation, the distance perception system was expected to take reading from shifting, rippling, flexing human body parts. Body parts which may be clothed, shaved, hairy, firm, or soft. Body parts with rounded uneven surfaces at close ranges.

The conditions of operation featured many unknowns and the specific approach selected for the actuators could not be known prior to selection of the proximity sensing method (the significant delays would have been untenable). As such, the

possibility of acoustic noise in the actuation system or the environment in general could not be dismissed.

Given this understanding of the operating conditions, ultrasonic sensors were considered inappropriate for the creation of a robust design within the constraints of the project.

IR range sensing was selected as the approach for determining distance. The Vishay TCRT5000 - Reflective Optical Sensor with Transistor Output was selected for the IR range sensing (Vishay Semiconductors, 2017), see Figure 15: TRCT5000. As stated by the manufacturer "The TCRT5000 and TCRT5000L are reflective sensors which include an infrared emitter and phototransistor in a leaded package which blocks visible light. The package includes two mounting clips." (Vishay Semiconductors, 2017).

Figure 15: TRCT5000 (Vishay Semiconductors, 2017)

The TCRT5000's datasheet may be found in the attached documents as "TCRT5000 - Reflective Optical Sensor with Transistor Output.pdf". The following circuit was used for the configuration of the TRCT5000s within the project, see Figure 16: TRCT5000 Topology, where **SIG** represents the output signal.
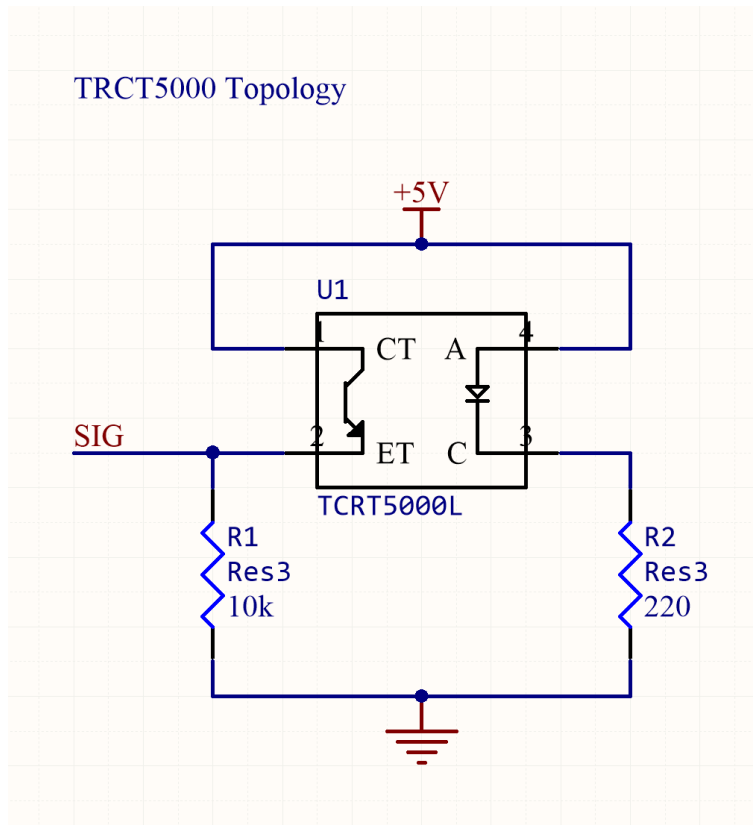
Figure 16: TRCT5000 Topology

A printed circuit board (PCB) would be created to which an IR transceiver, or emitter and receiver, could be mounted. The PCB would be designed as such that it would interface with external systems by only power and signal cables. Ideally, the IR PCB would be modular, and in the case of damage, simply replaced with another like it. This circuit board would feature the circuit in Figure 16: TRCT5000 Topology and the header depicted in Figure 17: IR Sensor Mount Header Topology.
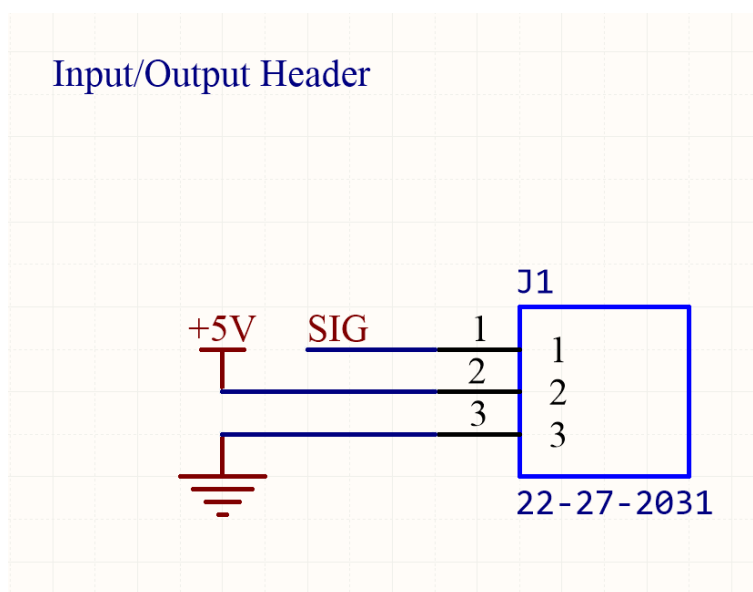
Figure 17: IR Sensor Mount Header Topology

The PCB was designed in Altium Designer (16.1), the PCB schematic may be found in the attached documents under the designation "IR Sensor Mount" and shown in Figure 18: IR Sensor Mount PCB Depiction.
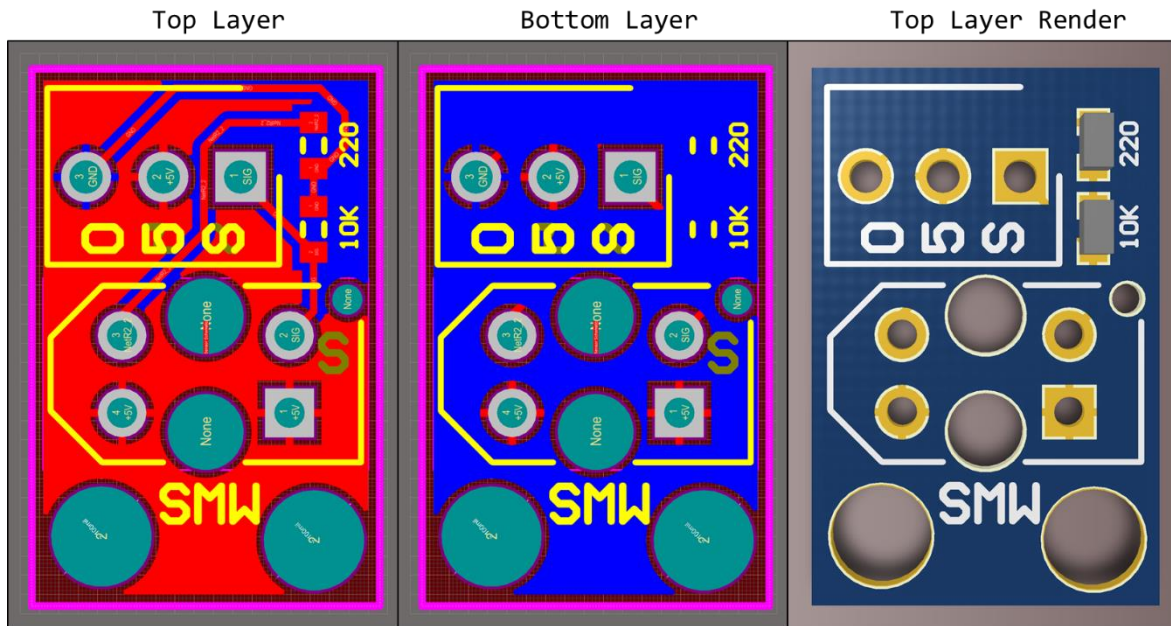
Figure 18: IR Sensor Mount PCB Depiction

The PCBs were fabricated and assembled as shown in Figure 19: Fabricated IR Sensor Mount PCB.

Kt

Figure 19: Fabricated IR Sensor Mount PCB

9.3.2 Fixed Rotational Axis

The fixed rotational axis upon which distance measurements would be referenced was determined to be the hip, knee, and ankle joints where ostensibly the actuators axis were to be place. As noted in 11, this considerable simplifies the kinematics and controls of the system. However, as the size of the exoskeleton and the limb segments devised was dependent on the mechanical build by those responsible for the actuation system estimations where required for the majority of the project regarding the specific length of limbs.

While it was presumed the exoskeleton's structural systems would be on the external sides of the pilot's body, the mounts for the position detection system would be designed without specifies on materials or dimensions of the exoskeleton (these values would remain unconfirmed until exceedingly late within the project).

It could not be presumed that the exoskeleton segments would have free ends, so the system would need to be designed to be attached, firmly, to a rod of an arbitrary shaped cross section of an arbitrary size, without access to a free end. It was required that wobbling vibration, ro movement of any kind was to be minimised

and the connection would be remove and reattached an indeterminant number of times. The connection needed to be fast, simple, and not so complicated to introduce risks of improper application.

Hose clamps were identified as a suitable fastener method. Screw/band (worm gear) clamps, see Figure 20: Hose Clamp, are reusable, can be applied to a rod of an arbitrary shape and size (with ranges), affix firmly, and may be attached quickly with a screwdriver.

Figure 20: Hose Clamp (Bunnings, 2018)

However, as the details of the proposed exoskeleton became available it was noted that the cross section of exoskeleton frame may have been as small as 5mm in diameter. A size below the range of standard hose clamps. Instead, cable ties were identified as an ideal fastener method.

Seen in Figure 21: Cable Tie, cable ties, or zip ties are a form of typically plastic ratcheting strap. The can be affixed to a rod of an arbitrary shape and size, attached by hand, and are disposable. While a less permanent solution for an attachment mechanism compared to hose clamps, the were deemed sufficient for a proof of concept.

Figure 21: Cable Tie (Computer Cable Store, 2018)

To mount the measurement structure to the exoskeleton a plat was design that could sit flush to the frame. As seen in figure Figure 22: Mount Structure, the structure (black), could be mounted to the exoskeleton frame A. Seen from the side, gutters where placed (B) so cable ties could be affixed, while guard rails (C) ensured the cable ties did not slip or move during operation. The measurement structure and any auxiliary objects could be affixed at the surface of the plate (D) with

counterbored sections (E) for nuts and bolts to be mounted while sitting flush with the surface of the exoskeleton.
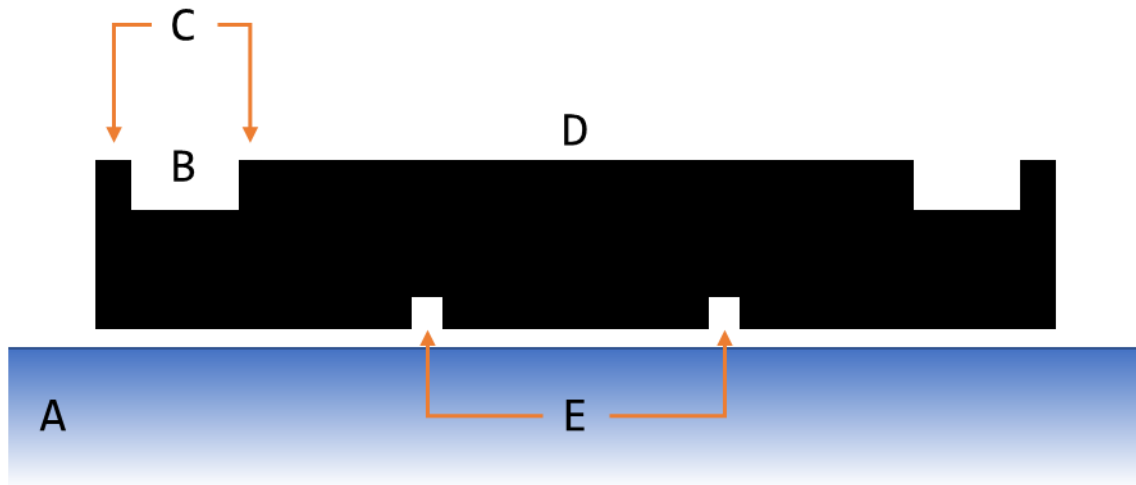
Figure 22: Mount Structure

The component was created in Autodesk Inventor, as seen in Figure 23: Mount Structure (Single) CAD. Attached to this document full CAD files for all components can be found kt.

Kt

Figure 23: Mount Structure (Single) CAD

To minimise the weight of this component and ease in manufacturing, the mounting plate was constructed via 3D printing, see Figure 24: Printed Mount Structure (Single).

kt

Figure 24: Printed Mount Structure (Single)

Presuming a fixed mounting place (as given by the mount structure) a scaffolding structure would be required to mount the IR sensor PCBs in place. After testing the effective range of the IR sensors created it was determined that two sensors working in tandem provided the most reliable measurements of position. Two sensors doubled the effective IR emitted, and given the irregular surfaces of the human body, the readings could be averaged to give a more consistent reading.

In the circumstance of trying to maintain a consistent offset from the pilot, as noted in kt (controls), the goals of the control systems is not to maintain an exact distance from the pilot, but maintain the safe distance on either side of the pilot. Rather than a solution comprised of measuring the pilot and attempting to maintain a specific offset, sensors on either side of the pilot could be used to detect the difference in the offset on both sides.

The design depicted in Figure 25: Sensor Frame was created. The frame (B) would envelope the pilot (A), and attach to the mount structure (F), see Figure 22: Mount Structure, on the outside edge of the pilot. A pair of sensors would detect in tandem (C) on either side the pilot (D), effectively measuring the position of the front and back of their leg in relation to the actuation of the exoskeleton.
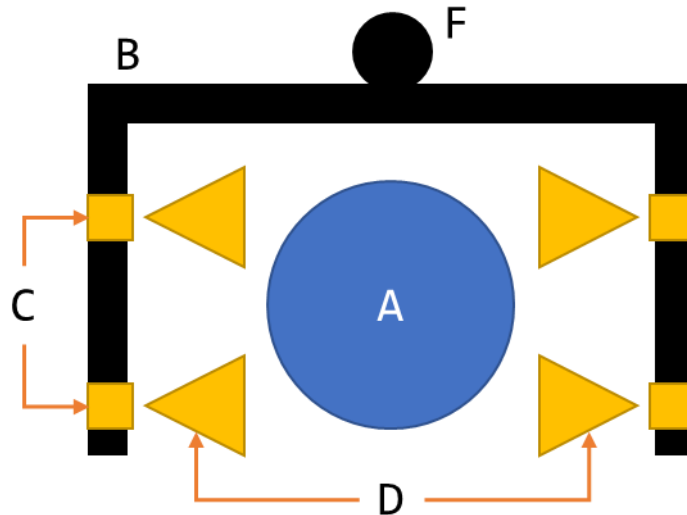
Figure 25: Sensor Frame

As shown in Figure 26: Constructed Sensor Frame, the sensor frame was constructed from aluminium, and later wood. Aluminium was selected for is strength and weight (relative to other metals). Once tested using the rig developed in 13, a lighter material was sought. Wood was selected. While adequate for a prototype, the materials used should be replaced with lighter plastic or carbon fibre materials for future designs; the structural requirements of the system are minimal and weight reduction is a priority.

kt

Figure 26: Constructed Sensor Frame

9.3.3 Mapping Values
kt

9.4 Results and Discussion
The final system was commissioned and assembled, as shown in Figure 27: Subsystem One (Assembled) .

Figure 27: Subsystem One (Assembled)

How well did it work?

10 Subsystem Two: Force applied by and to Exoskeleton

This section details the analysis, design, implementation, and results of the subsystem responsible for the perception of the applied by the exoskeleton to the environment and by the pilot to the exoskeleton.

10.1 Requirements and Functional Decomposition

The overarching purpose of subsystem two (SS2) is to measure the force applied to the internals and externals of the suit.
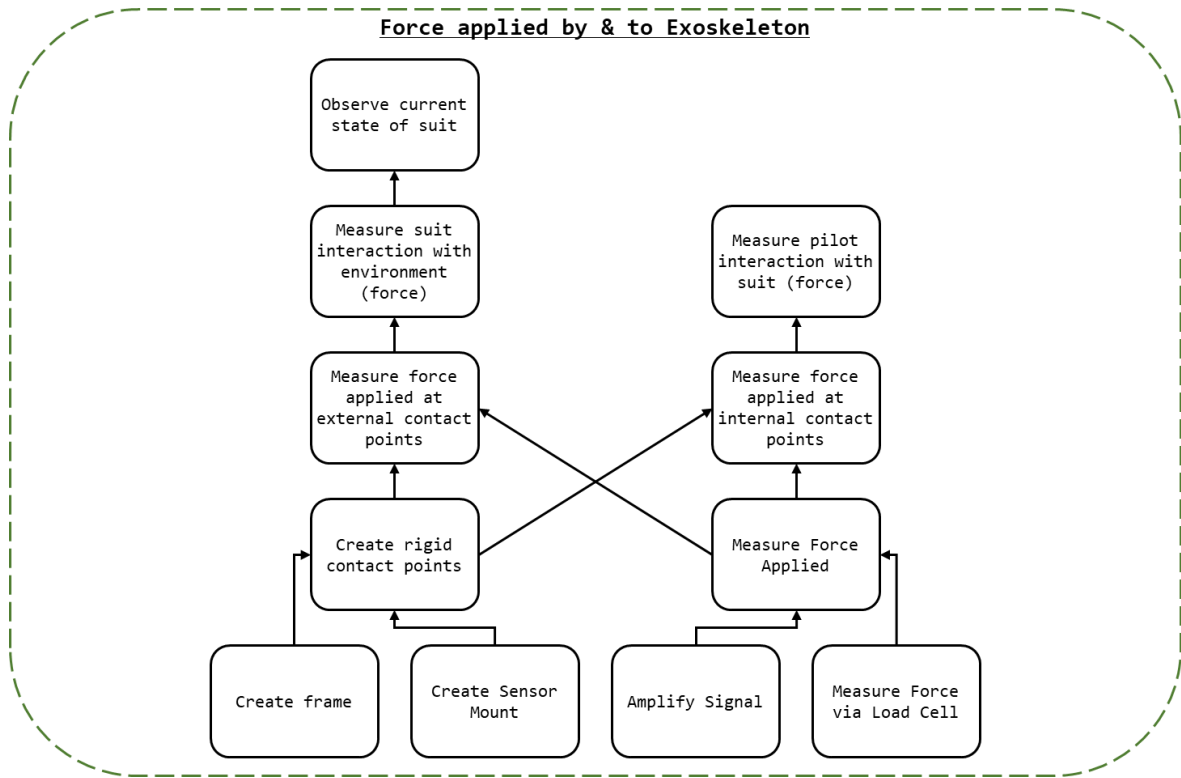
Figure 28: SS2 Breakdown

As seen in Figure 28: SS2 Breakdown, to measure the force applied to the suit at the designated contact points (feet and upper thigh) the following was required:

- Creating of rigid contact point upon which force application could be measured;
  - o This would require a rigid frame upon which sensors could be mounted; and,
  - o Mounts for force sensors.
- Measuring the force applied to the surface; and,
  - o This would involve measuring the force applied via load cell; and,
  - o Amplifying the signal from the load cells.
- The measured distance must be parsed from raw values into useable data.
  - o functionally, this is the process of deriving the function that maps raw analogue voltage values to force.

10.2 Background and Prior Art

10.2.1 Load Cells

Transducers are "elements that convert from one form of energy to another for example, sound to electricity" (Agarwal, 2005). A load cell is a type of transducer that converts the application of force or pressure into voltage or a change in imprudence. A load cell may be effectively used to measure the force applied to a surface, and the fundamental technology behind the common bathroom scale.

10.3 Approach and Execution

10.3.1 Measure Force

Load cells would be used to measure the force application to the contact points. Load cells allow for the précised measurement of force application in real time. Given the weight of the individuals associated with the project and preliminary estimations of the exoskeleton mass it was assumed that the mass for the entire system and pilot would not exceed 150 kg. Due to the incrementation of load cell ratings, 200 kg (four 50kg load cells) were selected. As seen in Figure 29: YZC-161B - 50kg Load Cell, the YZC-161B 50kg (coincidentally the load cell used in bathroom scales) is a flat strain-gauge type load cell specifically rated for human mass measurement.

Figure 29: YZC-161B - 50kg Load Cell (ZJIA, 2018)

The YZV-161B's datasheet may be found in the attached documents as "YZC-161B - 50kg Load Cell.pdf". The designation of each wire for the YZC-161B may be found in Figure 30: YZC-161B Wire Configuration.
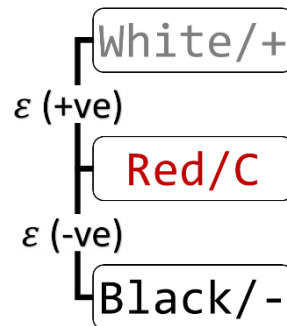
Figure 30: YZC-161B Wire Configuration

Four YZC-161B were wired in Wheatstone bridge configuration as shown in Figure 31: Load Cell Configuration.
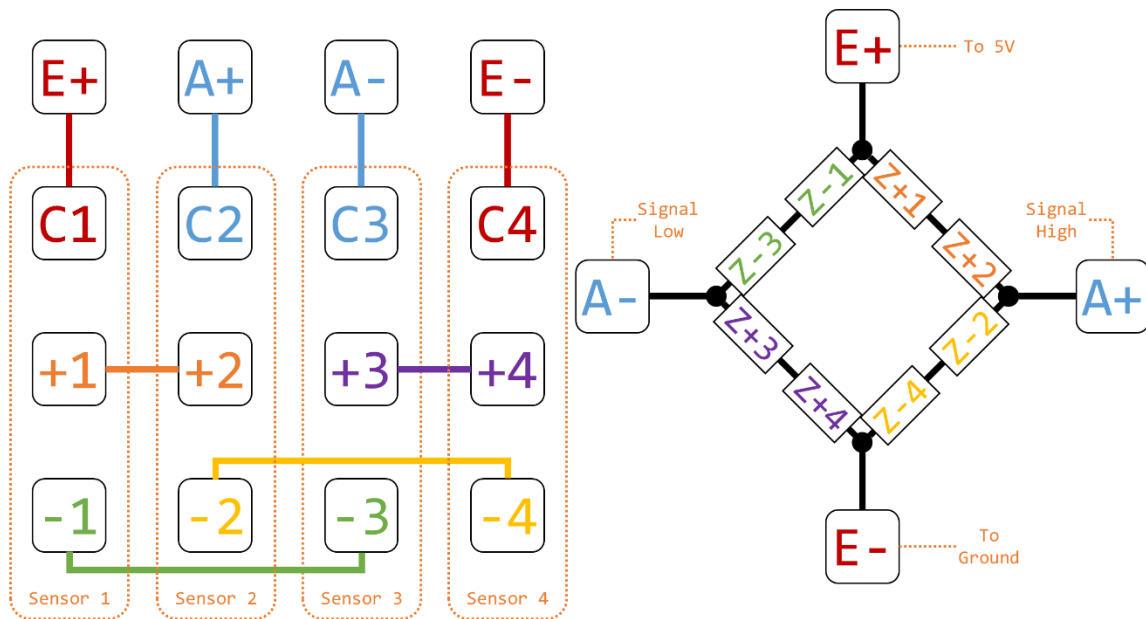
Figure 31: Load Cell Configuration

The configuration shown in Figure 31: Load Cell Configuration was implement in the PCB design of the controller boards, detailed in kt, in the schematic shown in Figure 32: Load Cell Topology, where B and T refer to the external and internal (bottom and top) load cell sets respectively.
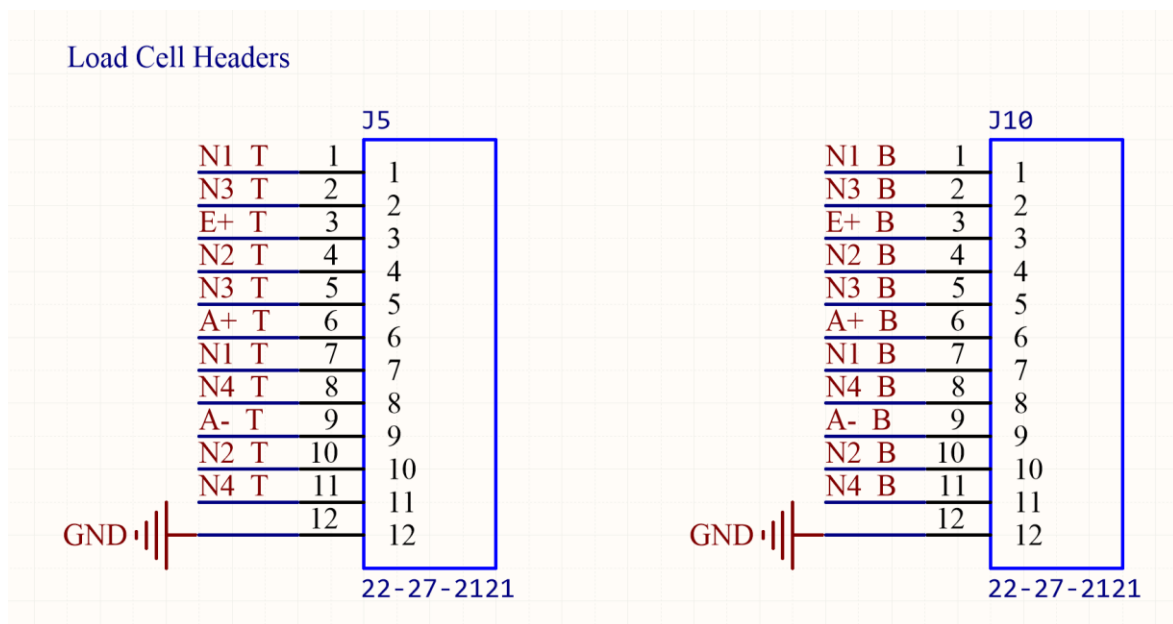
Figure 32: Load Cell Topology

10.3.2 Amplify Signal

To measure the signal output by the Wheatstone bridge configuration an instrumentation amplifier was used. The amplifier selected was the INA125, as seen in Figure 33: INA125 - Instrumentation Amplifier.

Figure 33: INA125 - Instrumentation Amplifier

The INA125's datasheet may be found in the attached documents as "INA125 - Instrumentation Amplifier With Precision Voltage Reference.pdf". The INA125s in the project were wired as depicted in Figure 34: Load Cell Amplifier Topology.
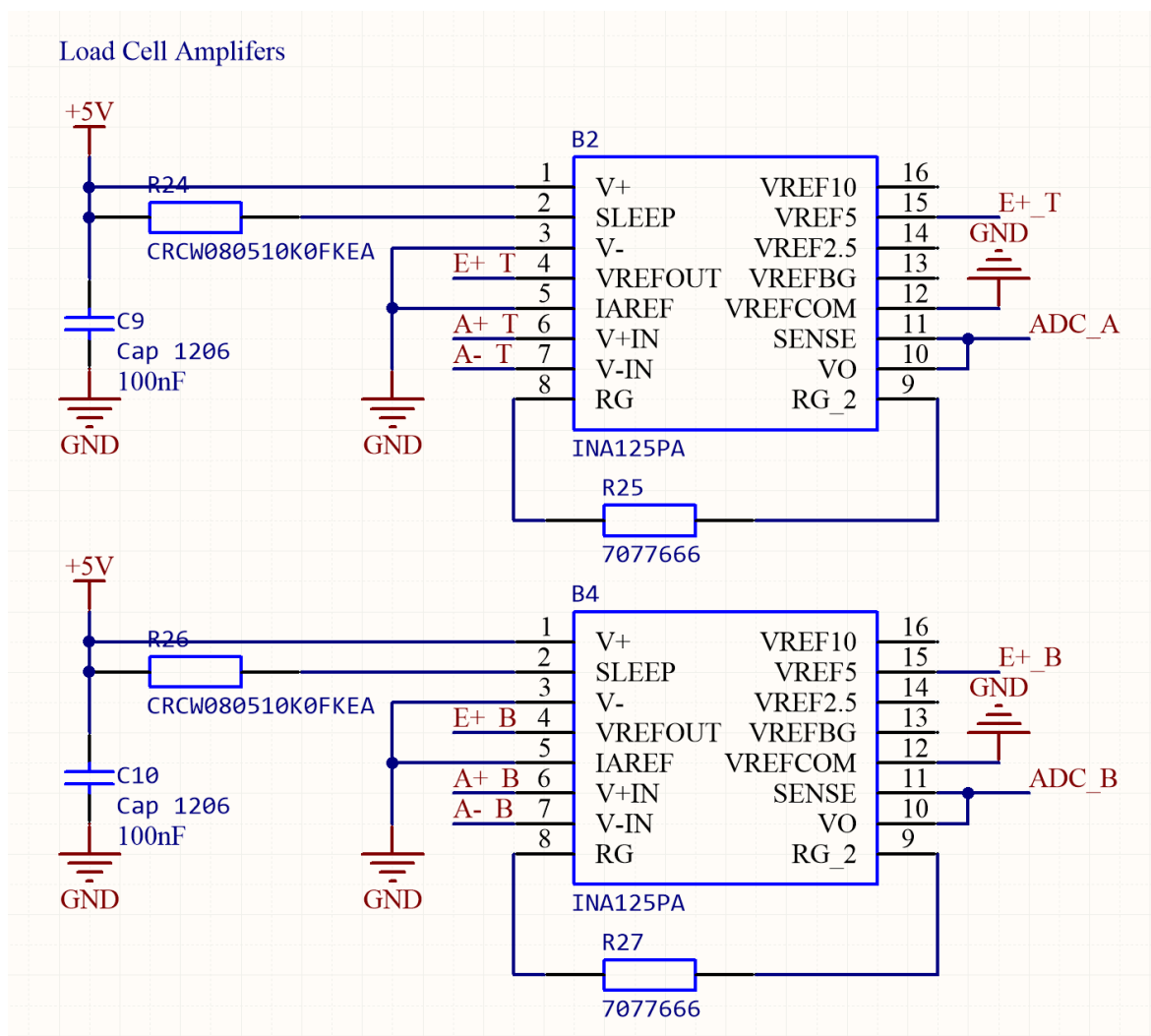
Figure 34: Load Cell Amplifier Topology

The INA125 allows for adjustable gain determined by the value of R_G, shown as R25 and R27 in Figure 34: Load Cell Amplifier Topology. The gain of the amplifier was given by Equation 7: INA125 Gain.

$$G = 4 + \frac{60 \, k\Omega}{R_G}$$

Equation 7: INA125 Gain

Alas, the quality control for the YZC-161B was terrible. The gain required could not be determined in advance. This may have been the consequence of buying cheap Shenzhen part. As seen in Table 3: Load Cell Calibration for two sensors set received in the same shipment, fresh from the packaging, the gain required for the same effective range of measurement was approximately ten times greater.

Instead, socket headers were attached to a calibration board in place of resistors (so resistors could be added and removed without soldering). A load cell could hen be attached to the board and calibrated, finding the resistor and gain that was most suitable.

As discussed in kt, the demonstration to be conducted would not include a fully constructed exoskeleton and demonstration rigs were to be created. Consequentially, rather than configuring the load cells for full force range expected by the system, instead the load cells were configured so that the force applied by human hands would be sufficient to trigger a system response.

To calibrate the load cells the following method was used:

1. Tare the load cells by recording the values taken at no weight applied;
2. Place a known weight on the load cells and record the readings;
3. Repeat step 2 with all available known weights; and,
4. Repeat steps 2 and 3 at least 3 times.

The results were then processed, and the relationship between the sensor readings and mass were determined. As seen in Figure 35: Load Cell Calibration Data, the relationship between the voltage output and the mass is linear. Note that the change in resistance of the load cells is directly proportional, and the voltage follows the opposite relationship.
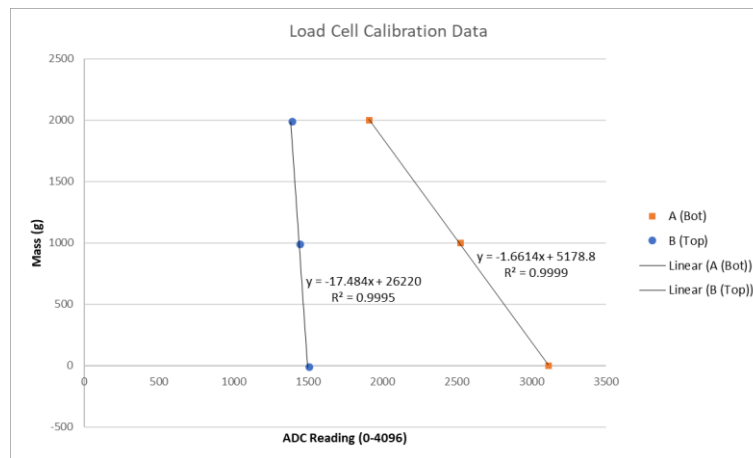
Figure 35: Load Cell Calibration Data

For the load cells used for the demonstration and test B, as detailed in kt (SS5) and kt (integrated) the configuration in Table 3: Load Cell Calibration was used.

Table 3: Load Cell Calibration

Load Cell Array	R_G	Gain	Voltage to Mass Function (as enacted in C)
Top (Internal)	4.7Ω	12800	massA = -1.6614 * ADC_A_Value + 5178.8;
Bottom (External)	47Ω	1280	massB = -17.484 * ADC_B_Value + 26220;

10.3.3 Mount Sensor

kt

10.3.4 Rigid Frame

A rigid frame was required to ensure proper demarcation between internal and external force application. The frame was also to serve as the mount for the load cell mounts. Two aluminium plates where used with screw holes as needed. As noted in kt (section above), the load cells sipped did not match their description and feature prefabricated feet; rather than discarding them they were integrated into the design.

The design for the rigid frame with load cells and mounts may be found in Figure 36: Force Sensor Configuration. A rigid centre plate separated the internal and external load cells. A rigid top plate was added to the internal edge of the rig to protect the load cells and ensure an evenly distributed force from the pilot. In the case where the pilot applied force to the environment (A) force applied would be transmitted to the internal load cells, but the external load cells would remain independent (receiving force only from obstacles. In the case were obstacles applied force but the pilot did not, the rigid plate would decouple the force allowing the controls system to indicate a stop condition.
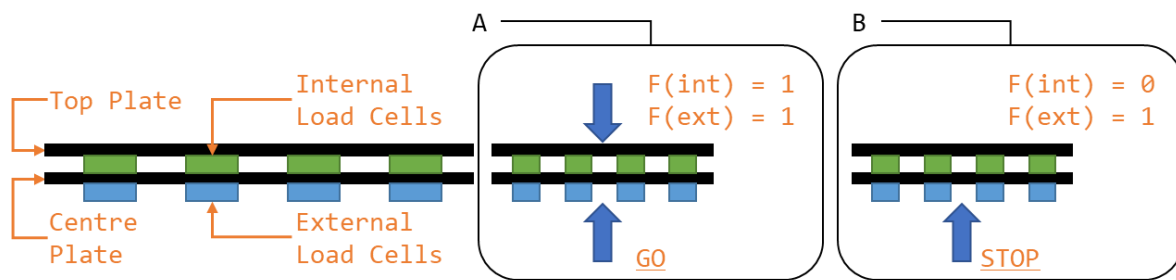
Figure 36: Force Sensor Configuration

10.4 Results and Discussion

Quality control on the YZC is dogshit

Gross vs fine motor control

Redo sensor mounts

11 Subsystem Three: Controls and Decision Making

This section details the analysis, design, implementation, and results of the subsystem responsible for determining the actions required by the actuation system.

11.1 Requirements and Functional Decomposition

The overarching purpose of subsystem three (SS3) was to determine the action that should be taken by the actuator system to minimise the error in the system.
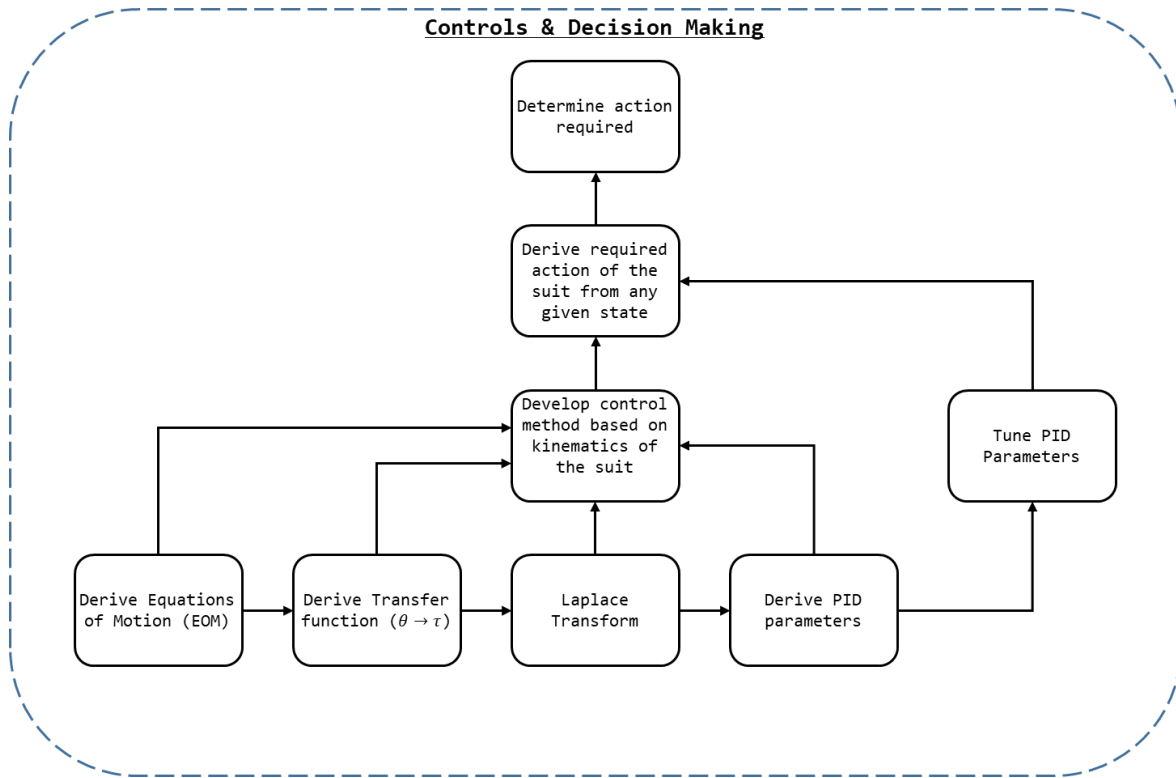
Figure 37: SS3 Breakdown

As seen in Figure 37: SS3 Breakdown, to determine the action required in a state (given by the values determined by SS1, SS2, and SS4) the action required in any given state must be known.

To determine the general solution of what actions should be taken at any given state the controls parameters and method for the system should be derived, and then this model should be refined by practically tuning the solution.

The methodology for tuning the controls parameters of the system is discussed in kt, but the initial values to be refined are best source directly from the theory.

To determine the control parameters for the system the following method is employed:

1. Derive the equations of motion (EOM) for the system;
2. From the EOM derive the transfer function (TF) of the system (torque (τ) with respect to angle (θ));

3. Transform the TF into the Laplace Domain; and,
4. Derive the PID parameters from the Laplace Domain TF.

Ultimately, five sets of controls were derived during the project: three for the 3 Degree of Freedom (DOF) lower extremity system (each joint had its own parameters), one for the continuous servomotor (which was abandoned as discussed in kt), and the positional servomotor.

The 3 DOF system was to control the lower extremity exoskeleton being constructed by the actuators and structural side of the project. However, as actual values for system parameters (masses, dimensions, moments of inertia, etc...) were never confirmed the solution had to be found algebraically.

The two systems used in testing featured their own embedded control systems, and their torque, angle, velocity, and acceleration could not be directly controlled. As such precise controls could not be derive from first principles. Instead the controls systems would need to be tuned empirically to achieve the desired system response.

11.2 Background and Prior Art

The goal of SS3 is to model the dynamics expected of the system, establish the manipulator equations of motion, and derive the appropriate controls structure to create the behaviour required, in a stable fashion.

11.2.1 Jacobian

For a system, in this case a manipulator, in the configuration given by the vector q there is corresponding psotion for the end-effector given by the vector x. The Jacobian matrix, J, describes the relationship between the time derivatives of q and x ($\dot{q}$ and $\dot{x}$ respectively). The Jacobian matrix, or simply the Jacobian, given by Equation 8, allows use to describe the system by Equation 9.

$$J = \begin{pmatrix} \dfrac{\partial x}{\partial \theta_1} & \dfrac{\partial x}{\partial \theta_2} & \dfrac{\partial x}{\partial \theta_3} \\ \dfrac{\partial y}{\partial \theta_1} & \dfrac{\partial y}{\partial \theta_2} & \dfrac{\partial y}{\partial \theta_3} \\ \dfrac{\partial z}{\partial \theta_1} & \dfrac{\partial z}{\partial \theta_2} & \dfrac{\partial z}{\partial \theta_3} \end{pmatrix}$$

Equation 8: Jacobian

$$\dot{x} = J(q)\dot{q}$$

Equation 9: Relationship between q and x

Where $q = (\theta_1, \theta_2, \theta_3)$.

11.2.2 Dynamics

11.2.2.1 Explicit Form of the Equations of Motion

We begin with the Euler–Lagrange equations, or Lagrange's equations of the second kind, Equation 10.

$$\frac{d}{dt}\left(\frac{\partial L}{\partial \dot{q}}\right) - \frac{\partial L}{\partial q} = \tau$$

Equation 10: Euler–Lagrange equations (Khatib, 2008)

Where τ is the vector of applied generalised torques. The Lagrangian, L, is given by Equation 11.

$$L = K - V$$

Equation 11: The Lagrangian (Khatib, 2008)

Where V is the potential energy of the system, and K is the kinetic energy of the system. As seen in Equation 12, K may be given in terms of the generalised velocities, $\dot{q}$ (as seen in Equation 10: Euler–Lagrange equations) and the manipulator mass matrix M.

$$K = \frac{1}{2}\dot{q}^T M \dot{q}$$

Equation 12: Kinetic Energy (Khatib, 2008)

Through Equation 10 we may say that $\frac{\partial K}{\partial \dot{q}} = \frac{\partial}{\partial \dot{q}}\left(\frac{1}{2}\dot{q}^T M(q)\dot{q}\right) = M\dot{q}$

Equation 13and Equation 14 hold.

$$\frac{\partial K}{\partial \dot{q}} = \frac{\partial}{\partial \dot{q}}\left(\frac{1}{2}\dot{q}^T M(q)\dot{q}\right) = M\dot{q}$$

Equation 13: Kinetic Energy Partial Derivative

$$\frac{d}{dt}\left(\frac{\partial K}{\partial \dot{q}}\right) = M\ddot{q} + \dot{M}\dot{q}$$

Equation 14: Kinetic Energy Time Derivative

Thus the inertial forces of Equation 11 may be expressed as Equation 15, where v is the vector of centrifugal and Coriolis forces, Equation 16.

$$\frac{d}{dt}\left(\frac{\partial K}{\partial \dot{q}}\right) - \frac{\partial K}{\partial q} = M\ddot{q} + \dot{M}\dot{q} - \frac{1}{2}\begin{bmatrix} \dot{q}^T \frac{\partial M}{\partial q_1}\dot{q} \\ \vdots \\ \dot{q}^T \frac{\partial M}{\partial q_n}\dot{q} \end{bmatrix} = M\ddot{q} + v(q, \dot{q})$$

Equation 15: Inertial Forces

$$v(q, \dot{q}) = \dot{M}\dot{q} - \frac{1}{2}\begin{bmatrix} \dot{q}^T \frac{\partial M}{\partial q_1}\dot{q} \\ \vdots \\ \dot{q}^T \frac{\partial M}{\partial q_n}\dot{q} \end{bmatrix} = C(q)[\dot{q}^2] + B(q)[\dot{q}\dot{q}]$$

Equation 16: Vector of centrifugal and Coriolis forces

Through Equation 15 we may yield the explicit form of the equations of motion (EOM), see Equation 17. Where g is the vector of gravity force and v is the vector of centrifugal and Coriolis forces. Equation 17, once found, may be used to map the relationship between the torque applied by the systems actuators and the resulting system configuration.

$$M(q)\ddot{q} + v(q,\dot{q}) + g(q) = \tau$$

Equation 17: Explicit form of EOM

11.2.2.2 Explicit form of Manipulator Mass Matrix

Kinetic energy is subject to the adaptive property (Siciliano & Khatib, 2016), and thus the total kinetic energy of a system is the summation of the kinetic energy of its links. Links here refers to the actuated limb segments of the exoskeleton correlating with the thigh, shin, and foot.

The kinetic energy of each link is comprised of a rotational and linear motion component. For a link with linear motion of v_{C_i}, an angular motion of ω_i, and an inertia tensor of I_{C_i}, the kinetic energy of the link , K_i, is given by Equation 18Equation 18. Where C_i refers to the centre of mass of the link.

$$K_i = \frac{1}{2}\left(m_i v_{C_i}^T v_{C_i} + \omega_i^T I_{C_i} \omega_i\right) = \frac{1}{2}\left(m_i \dot{q}^T J_{vi}^T J_{vi} \dot{q} + \dot{q}^T J_{\omega i}^T I_{C_i} J_{\omega i} \dot{q}\right)$$

Equation 18: Kinetic Energy of Link i

Given Equation 18 and the additive property it may be said that the kinetic of the system in total is given by Equation 19

$$K = \sum_{i=1}^{n} K_i$$

Equation 19: Kinetic energy of System

Using Equation 18 and Equation 19, factoring out $\dot{q}$, we develop Equation 20

$$K = \frac{1}{2}\sum_{i=1}^{n}\left(m_i \dot{q}^T J_{vi}^T J_{vi} \dot{q} + \dot{q}^T J_{\omega i}^T I_{C_i} J_{\omega i} \dot{q}\right) = \frac{1}{2}\dot{q}^T\left[\sum_{i=1}^{n}\left(m_i J_{vi}^T J_{vi} + J_{\omega i}^T I_{C_i} J_{\omega i}\right)\right]\dot{q}$$

Equation 20: Kinetic Energy of Total System

Equating Equation 20 to Equation 12 we find the Explicit form of Manipulator Mass Matrix, Equation 21.

$$M = \sum_{i=1}^{n}\left(m_i J_{vi}^T J_{vi} + J_{\omega i}^T I_{C_i} J_{\omega i}\right)$$

Equation 21: Explicit form of Manipulator Mass Matrix

11.2.2.3 Vector of centrifugal and Coriolis forces

We begin with Equation 16: Vector of centrifugal and Coriolis forces.

$$v(q, \dot{q}) = \dot{M}\dot{q} - \frac{1}{2}\begin{bmatrix} \dot{q}^T \dfrac{\partial M}{\partial q_1}\dot{q} \\ \vdots \\ \dot{q}^T \dfrac{\partial M}{\partial q_n}\dot{q} \end{bmatrix} = C(q)[\dot{q}^2] + B(q)[\dot{q}\dot{q}]$$

Sparing the derivation, we can say that givem Equation 22 and Equation 23, that Equation 24 and Equation 25 hold true.

$$m_{ijk} = \frac{\partial m_{ij}}{\partial q_k}$$

Equation 22: mijk

$$b_{ijk} = \frac{1}{2}(m_{ijk} + m_{ikj} - m_{jki})$$

Equation 23: Christoffel Symbols

$$C(q) = \begin{bmatrix} b_{111} & b_{122} & \dots & b_{1nn} \\ b_{211} & b_{222} & \dots & b_{2nn} \\ \vdots & \vdots & \ddots & \vdots \\ b_{n11} & b_{n22} & \dots & b_{nnn} \end{bmatrix}$$

Equation 24: Coefficients associated with centrifugal forces

$$B(q) = \begin{bmatrix} 2b_{112} & 2b_{113} & \dots & 2b_{11n} & 2b_{123} & \dots & 2b_{12n} & \dots & 2b_{1(n-1)n} \\ 2b_{212} & 2b_{213} & \dots & 2b_{21n} & 2b_{223} & \dots & 2b_{22n} & \dots & 2b_{2(n-1)n} \\ \vdots & \vdots & \vdots & \vdots & \vdots & \vdots & \vdots & \ddots & \vdots \\ 2b_{n12} & 2b_{n13} & \dots & 2b_{n1n} & 2b_{n23} & \dots & 2b_{n2n} & \dots & 2b_{n(n-1)n} \end{bmatrix}$$

Equation 25: Coefficients associated with Coriolis force

Where

$$[\dot{q}^2]^T = [\dot{q}_1{}^2 \quad \dot{q}_2{}^2 \quad \dots \quad \dot{q}_n^2]$$

$$[\dot{q}\dot{q}] = [\dot{q}_1\dot{q}_2 \quad \dot{q}_1\dot{q}_3 \quad \dots \quad \dot{q}_1\dot{q}_n \quad \dot{q}_2\dot{q}_3 \quad \dot{q}_2\dot{q}_4 \quad \dots \quad \dot{q}_2\dot{q}_n \quad \dots \quad \dot{q}_{(n-1)}\dot{q}_n]$$

11.2.2.4 Vector of gravity force

The vector of gravity force, g, represents the gravitational potential energy of the system. The gravitational potential energy of the system is given by the gravitational potential energy of every link in the system, see Equation 26.

$$V = \sum_{i=1}^{n} V_i$$

Equation 26: Potential Energy of the System

The gravitational potential energy of each link is given by Equation 27, where is the height of the centre of mass of the link relative to the origin (pelvis).

$$V_i = m_i g h$$

Equation 27: Gravitational Potential Energy of Each Link

Thus, we may say (using the Jacobian to map the location) the vector of gravity force, g, is given by Equation 28.

$$g = -\begin{pmatrix} J_{v1}^T & J_{v2}^T & J_{v3}^T \end{pmatrix} \begin{pmatrix} m_1 g \\ m_2 g \\ m_3 g \end{pmatrix}$$

Equation 28: Vector of Gravity Force

11.3 Approach and Execution

Before the kinematics of the system could be found, the exoskeleton needed to be abstracted into a model. Consider the following:

a) The exoskeleton is to be affixed to the lower torso of the pilot;
b) The pilot is presumed to maintain the balance of the system using their body;
c) The pilot should be able to manipulate the legs of the system independently;
d) The legs, while part of the same exoskeletons, are essentially fixed at the pelvis and operate independently; and,
e) We may therefore consider each leg as an independent manipulator with a fixed reference frame at the pelvis.

As noted in kt, each joint of the exoskeleton shall be constrained to 1 DOF. Therefore, we may abstract the exoskeleton as two 3 DOF RRR manipulators, as seen in Figure 38: Exoskeleton Abstraction.
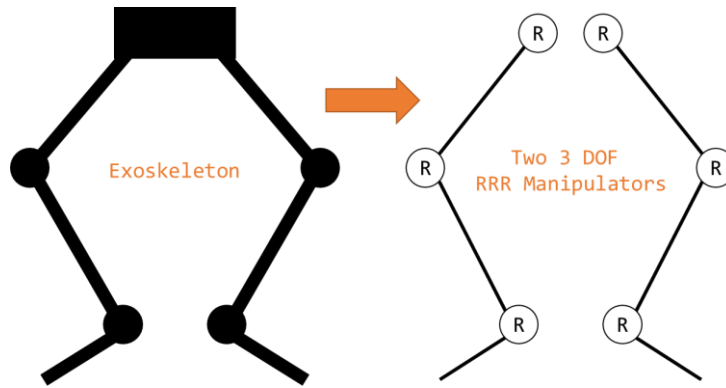

Figure 38: Exoskeleton Abstraction

For modelling the system, the parameters seen in Figure 39: 3 DOF RRR Parameterisation shall be used. Note angle shall be measured relative to the previous link with a clockwise positive convention.
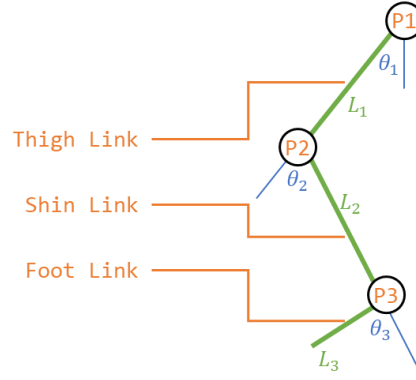
Figure 39: 3 DOF RRR Parameterisation

As noted in kt (requirements section) the actual values for the exoskeleton were never confirmed and the controls had to be completed symbolically. On one hand, this resulted in a general solution that can be applied to any 3 DOF RRR serial manipulator. On the other hand, the equations become cumbersome and large. As a result, many of the equations shall be taken to their general form, as explicit solutions shall be left as an exercise to the reader.

11.3.1 Jacobian

To find the Jacobian of a 3 DOF Revolute Manipulator:

$$v = System\ Velocity$$

$$^0v_{P_1} = \omega_1 * P_1$$

$$^0v_{P_2} = {^0v_{P_1}} + \omega_2 * P_2$$

$$^0v_{P_3} = {^0v_{P_2}} + \omega_3 * P_3$$

Or, for a system at low velocity (i.e. standing, squatting, sitting, stairs, walking):

$$^0v_{P_1} = \begin{bmatrix} 0 & -\dot{\theta}_1 & 0 \\ \dot{\theta}_1 & 0 & 0 \\ 0 & 0 & 0 \end{bmatrix} \begin{bmatrix} L_1c_1 \\ L_1s_1 \\ 0 \end{bmatrix} = \begin{bmatrix} -L_1s_1 \\ L_1c_1 \\ 0 \end{bmatrix} \dot{\theta}_1$$

$$^0v_{P_2} = {^0v_{P_1}} + \begin{bmatrix} 0 & -(\dot{\theta}_1 + \dot{\theta}_2) & 0 \\ (\dot{\theta}_1 + \dot{\theta}_2) & 0 & 0 \\ 0 & 0 & 0 \end{bmatrix} \begin{bmatrix} L_2c_{12} \\ L_2s_{12} \\ 0 \end{bmatrix} = \begin{bmatrix} -L_1s_1 \\ L_1c_1 \\ 0 \end{bmatrix} \dot{\theta}_1 + \begin{bmatrix} -L_2s_{12} \\ L_2c_{12} \\ 0 \end{bmatrix} (\dot{\theta}_1 + \dot{\theta}_2)$$

$$^0v_{P_2} = {^0v_{P_1}} + {^0v_{P_2}} + \begin{bmatrix} 0 & -(\dot{\theta}_1 + \dot{\theta}_2 + \dot{\theta}_3) & 0 \\ (\dot{\theta}_1 + \dot{\theta}_2 + \dot{\theta}_3) & 0 & 0 \\ 0 & 0 & 0 \end{bmatrix} \begin{bmatrix} L_3c_{123} \\ L_3s_{123} \\ 0 \end{bmatrix}$$

$$= \begin{bmatrix} -L_1s_1 \\ L_1c_1 \\ 0 \end{bmatrix} \dot{\theta}_1 + \begin{bmatrix} -L_2s_{12} \\ L_2c_{12} \\ 0 \end{bmatrix} (\dot{\theta}_1 + \dot{\theta}_2) + \begin{bmatrix} -L_3s_{123} \\ L_3c_{123} \\ 0 \end{bmatrix} (\dot{\theta}_1 + \dot{\theta}_2 + \dot{\theta}_3)$$

In matrix form

$$^0v_{P_1} = \begin{bmatrix} -l_1 s_1 & 0 & 0 \\ l_1 c_1 0 & 0 & 0 \\ 0 & 0 & 0 \end{bmatrix} \begin{bmatrix} \dot{\theta}_1 \\ \dot{\theta}_2 \\ \dot{\theta}_3 \end{bmatrix}$$

$$^0v_{P_2} = \begin{bmatrix} -(l_1 s_1 + l_2 s_{12}) & -l_2 s_{12} & 0 \\ l_1 c_1 + l_2 c_{12} & -l_2 c_{12} & 0 \\ 0 & 0 & 0 \end{bmatrix} \begin{bmatrix} \dot{\theta}_1 \\ \dot{\theta}_2 \\ \dot{\theta}_3 \end{bmatrix}$$

$$^0v_{P_2} = \begin{bmatrix} -(l_1 s_1 + l_2 s_{12} + l_3 s_{123}) & -(l_2 s_{12} + l_3 s_{123}) & -l_3 s_{123} \\ l_1 c_1 + l_2 c_{12} + l_3 c_{123} & -l_2 c_{12} + l_3 c_{123} & l_3 c_{123} \\ 0 & 0 & 0 \end{bmatrix} \begin{bmatrix} \dot{\theta}_1 \\ \dot{\theta}_2 \\ \dot{\theta}_3 \end{bmatrix}$$

The angular velocities are simply additive:

$$^0\omega_1 = \begin{bmatrix} 0 & 0 & 0 \\ 0 & 0 & 0 \\ 1 & 0 & 0 \end{bmatrix} \begin{bmatrix} \dot{\theta}_1 \\ \dot{\theta}_2 \\ \dot{\theta}_3 \end{bmatrix}$$

$$^0\omega_2 = \begin{bmatrix} 0 & 0 & 0 \\ 0 & 0 & 0 \\ 1 & 1 & 0 \end{bmatrix} \begin{bmatrix} \dot{\theta}_1 \\ \dot{\theta}_2 \\ \dot{\theta}_3 \end{bmatrix}$$

$$^0\omega_3 = \begin{bmatrix} 0 & 0 & 0 \\ 0 & 0 & 0 \\ 1 & 1 & 1 \end{bmatrix} \begin{bmatrix} \dot{\theta}_1 \\ \dot{\theta}_2 \\ \dot{\theta}_3 \end{bmatrix}$$

From which we obtain the Jacobian of a 3 DOF Revolute Manipulator, as seen in Equation 29.

$$\begin{pmatrix} v \\ \omega \end{pmatrix} = J \begin{pmatrix} \dot{\theta}_1 \\ \dot{\theta}_2 \\ \dot{\theta}_3 \end{pmatrix}$$

Equation 29: 3 DOF Revolute Manipulator Jacobian

11.3.2 Dynamics

For a 3 DOF Revolute Manipulator where the inertia tensors of the links are I_1, I_2, and I_3 (Equation 30).

$$^1I_1 = \begin{pmatrix} I_{xx1} & 0 & 0 \\ 0 & I_{yy1} & 0 \\ 0 & 0 & I_{zz1} \end{pmatrix} \And\ ^2I_2 = \begin{pmatrix} I_{xx2} & 0 & 0 \\ 0 & I_{yy2} & 0 \\ 0 & 0 & I_{zz2} \end{pmatrix} \And\ ^3I_3 = \begin{pmatrix} I_{xx3} & 0 & 0 \\ 0 & I_{yy3} & 0 \\ 0 & 0 & I_{zz3} \end{pmatrix}$$

Equation 30: Inertia Tensors

11.3.2.1 *Explicit form of Manipulator Mass Matrix*

The mass matrix for the 3 DOF Revolute Manipulator is given by Equation 31. This process was completed with symbolic variables in MATLAB R2017b, as detailed in the attached files (get_EOM.m) kt.

$$M = m_1 J_{v1}^T J_{v1} + J_{\omega1}^T I_1 J_{\omega1} + m_2 J_{v2}^T J_{v2} + J_{\omega2}^T I_2 J_{\omega2} + m_3 J_{v3}^T J_{v3} + J_{\omega3}^T I_3 J_{\omega3}$$

Equation 31: Mass Matrix for the 3 DOF Revolute Manipulator

11.3.2.2 Vector of centrifugal and Coriolis forces

We begin with Equation 24.

$$C(q) = \begin{bmatrix} b_{111} & b_{122} & \cdots & b_{1nn} \\ b_{211} & b_{222} & \cdots & b_{2nn} \\ \vdots & \vdots & \ddots & \vdots \\ b_{n11} & b_{n22} & \cdots & b_{nnn} \end{bmatrix}$$

$$C(q) = \begin{bmatrix} b_{111} & b_{122} & b_{133} \\ b_{211} & b_{222} & b_{233} \\ b_{311} & b_{322} & b_{333} \end{bmatrix}$$

$$C(q) = \begin{bmatrix} 0 & \frac{1}{2}(m_{122} + m_{122} - m_{221}) & \frac{1}{2}(m_{133} + m_{133} - m_{331}) \\ \frac{1}{2}(m_{211} + m_{211} - m_{112}) & 0 & \frac{1}{2}(m_{233} + m_{233} - m_{332}) \\ \frac{1}{2}(m_{311} + m_{311} - m_{113}) & \frac{1}{2}(m_{322} + m_{322} - m_{223}) & 0 \end{bmatrix}$$

Equation 32: Vector of Centrifugal Forces

Next Equation 25.

$$B(q) = \begin{bmatrix} 2b_{112} & 2b_{113} & \cdots & 2b_{11n} & 2b_{123} & \cdots & 2b_{12n} & \cdots & 2b_{1(n-1)n} \\ 2b_{212} & 2b_{213} & \cdots & 2b_{21n} & 2b_{223} & \cdots & 2b_{22n} & \cdots & 2b_{2(n-1)n} \\ \vdots & \vdots & \vdots & \vdots & \vdots & \vdots & \vdots & \ddots & \vdots \\ 2b_{n12} & 2b_{n13} & \cdots & 2b_{n1n} & 2b_{n23} & \cdots & 2b_{n2n} & \cdots & 2b_{n(n-1)n} \end{bmatrix}$$

$$B(q) = \begin{bmatrix} 2b_{112} & 2b_{113} & 2b_{123} \\ 2b_{212} & 2b_{213} & 2b_{223} \\ 2b_{312} & 2b_{313} & 2b_{323} \end{bmatrix}$$

$$B(q) = \begin{bmatrix} m_{112} & m_{113} & (m_{123} + m_{132} - m_{231}) \\ 0 & (m_{213} + m_{231} - m_{132}) & m_{223} \\ (m_{312} + m_{321} - m_{123}) & 0 & 0 \end{bmatrix}$$

Equation 33: Vector of Coriolis Force

From Equation 23

$$b_{ijk} = \frac{1}{2}\left(m_{ijk} + m_{ikj} - m_{jki}\right) \rightarrow b_{iii} = b_{iji} = 0$$

Where

$$m_{ijk} = \frac{\partial m_{ij}}{\partial q_k}\left(m_{ij} = M_{ij}\right)$$

This process was completed with symbolic variables in MATLAB R2017b, as detailed in the attached files (get_EOM.m) kt.

11.3.2.3 Vector of gravity force

Continuing from Equation 28: Vector of Gravity Force

$$G = -\begin{pmatrix} J_{v1}^T & J_{v2}^T & J_{v3}^T \end{pmatrix} \begin{pmatrix} m_1 g \\ m_2 g \\ m_3 g \end{pmatrix}$$

$$G = -g(J_{v1}^T m_1 + J_{v2}^T m_2 + J_{v3}^T m_3)$$

Equation 34: Gravity Vector

Given J_{vi}^T, see Equation 29, we may find Equation 35.

$$G = -\left(\begin{bmatrix} -l_1 s_1 & l_1 c_1 & 0 \\ 0 & 0 & 0 \\ 0 & 0 & 0 \end{bmatrix} \begin{bmatrix} 0 \\ -m_1 g \\ 0 \end{bmatrix} + \begin{bmatrix} -(l_1 s_1 + l_2 s_{12}) & l_1 c_1 + l_2 c_{12} & 0 \\ -l_2 s_{12} & -l_2 c_{12} & 0 \\ 0 & 0 & 0 \end{bmatrix} \begin{bmatrix} 0 \\ -m_2 g \\ 0 \end{bmatrix} \right.$$

$$\left. + \begin{bmatrix} -(l_1 s_1 + l_2 s_{12} + l_3 s_{123}) & l_1 c_1 + l_2 c_{12} + l_3 c_{123} & 0 \\ -(l_2 s_{12} + l_3 s_{123}) & -l_2 c_{12} + l_3 c_{123} & 0 \\ -l_3 s_{123} & l_3 c_{123} & 0 \end{bmatrix} \begin{bmatrix} 0 \\ -m_3 g \\ 0 \end{bmatrix} \right)$$

$$G = \begin{bmatrix} ((m_1 + m_2 + m_3)l_1 c_1 + (m_2 + m_3)l_2 c_{12} + m_3 l_3 c_{123})g \\ ((m_2 + m_3)l_2 c_{12} + m_3 l_3 c_{123})g \\ (m_3 l_3 c_{123})g \end{bmatrix}$$

Equation 35: Vector of Gravity Force

This process was completed with symbolic variables in MATLAB R2017b, as detailed in the attached files (get_EOM.m) kt.

11.3.3 Explicit Form of the Equations of Motion

Base on Equation 31Equation 31: Mass Matrix for the 3 DOF Revolute Manipulator, Equation 32: Vector of Centrifugal Forces, Equation 33: Vector of Coriolis Force, and Equation 35: Vector of Gravity Force we may find the solution to Equation 17, as given by Equation 36

$$M(q)\ddot{q} + C(q)[\dot{q}^2] + B(q)[\dot{q}\dot{q}] + g(q) = \tau$$

Equation 36: Equations of Motion

This process was completed with symbolic variables in MATLAB R2017b, as detailed in the attached files (get_EOM.m) kt. The output of these equations, and the equations of motion for the system are as seen in Table 4: Equations of Motion.

Table 4: Equations of Motion

T1	dda2*(Izz2 + Izz3 + m3*(L2^2 + 2*cos(a3)*L2*l3 + L1*cos(a2)*L2 + l3^2 + L1*cos(a2 + a3)*l3) + l2*m2*(l2 + L1*cos(a2))) + dda3*(Izz3 + l3*m3*(l3 + L1*cos(a2 + a3) + L2*cos(a3))) - da1*(L1*da2*(l2*m2*sin(a2) + l3*m3*sin(a2 + a3) + L2*m3*sin(a2)) + da3*l3*m3*(L1*sin(a2 + a3) + L2*sin(a3))) - da2*(L1*(da1 + da2)*(l2*m2*sin(a2) + l3*m3*sin(a2 + a3) +

	L2*m3*sin(a2)) + da3*l3*m3*(L1*sin(a2 + a3) + L2*sin(a3))) + dda1*(Izz1 + Izz2 + Izz3 + L1^2*m2 + L1^2*m3 + L2^2*m3 + l1^2*m1 + l2^2*m2 + l3^2*m3 + 2*L1*l3*m3*cos(a2 + a3) + 2*L1*L2*m3*cos(a2) + 2*L1*l2*m2*cos(a2) + 2*L2*l3*m3*cos(a3)) + g*m2*(l2*cos(a1 + a2) + L1*cos(a1)) + g*m3*(L2*cos(a1 + a2) + L1*cos(a1) + l3*cos(a1 + a2 + a3)) + g*l1*m1*cos(a1) - da3*l3*m3*(L1*sin(a2 + a3) + L2*sin(a3))*(da1 + da2 + da3)
T2	dda1*(Izz2 + Izz3 + m3*(L2^2 + 2*cos(a3)*L2*l3 + L1*cos(a2)*L2 + l3^2 + L1*cos(a2 + a3)*l3) + l2*m2*(l2 + L1*cos(a2))) + da1*(L1*da1*(l2*m2*sin(a2) + l3*m3*sin(a2 + a3) + L2*m3*sin(a2)) - L2*da3*l3*m3*sin(a3)) + dda2*(Izz2 + Izz3 + m3*(L2^2 + 2*cos(a3)*L2*l3 + l3^2) + l2^2*m2) + dda3*(Izz3 + l3*m3*(l3 + L2*cos(a3))) + g*m3*(L2*cos(a1 + a2) + l3*cos(a1 + a2 + a3)) + g*l2*m2*cos(a1 + a2) - L2*da2*da3*l3*m3*sin(a3) - L2*da3*l3*m3*sin(a3)*(da1 + da2 + da3)
T3	dda3*(m3*l3^2 + Izz3) + dda1*(Izz3 + l3*m3*(l3 + L1*cos(a2 + a3) + L2*cos(a3))) + da1*(da1*l3*m3*(L1*sin(a2 + a3) + L2*sin(a3)) + L2*da2*l3*m3*sin(a3)) + dda2*(Izz3 + l3*m3*(l3 + L2*cos(a3))) + g*l3*m3*cos(a1 + a2 + a3) + L2*da2*l3*m3*sin(a3)*(da1 + da2)

Where

$$ai = \theta_i$$

$$dai = \dot{\theta_i}$$

$$ddai = \ddot{\theta_i}$$

$$Li = Length\ of\ Link$$

$$li = Distance\ from\ joint\ to\ center\ of\ mass\ of\ link$$

11.3.4 Laplace Transform

Once the equations of motion (EOM) had been found via MATLAB, the Laplace transform was performed on the EOM. Alas, MATLAB doesn't recognise the relationship between θ_i, $\dot{\theta_i}$, and $\ddot{\theta_i}$ for *syms*; they had to be treated as separate variables. Thus, the Laplace transform could not be applied outright. Instead, it would be performed manually by transforming each term individually through string manipulation (how MATLAB stores symbolic equations). This can be seen in detail in kt (get_EOM). But essentially boiled down to finding all instances of a variable (e.g. cos(a3)) and transforming it (e.g. 'A3*(s/(s^2 + 1))'). This of course had to happen from greatest term to smallest to avoid confusions in replacements (i.e. a3 includes dda3, da3, and a3, so it should be completed after all terms including dda3 and da3 are transformed.

While 3D laplace transforms are possible (Dawkins, 2018) it rather messy. Instead it will be assumed the behaviour of the systems in relation to a joint can be approximated to equal the behaviour of the system if the instantaneous state of

the rest of the joints is constant. This is to say, if we update θ_i sufficiently quickly/frequently we may treat changes in θ_j and θ_k as negligible.

The resulting equations may be found in Table 5: Laplace EOM.

Table 5: Laplace EOM

T1	`dda2*(m3*L2^2 + 2*m3*cos(a3)*L2*l3 + L1*m3*cos(a2)*L2 + m2*l2^2 + L1*m2*cos(a2)*l2 + m3*l3^2 + L1*m3*cos(a2 + a3)*l3 + Izz2 + Izz3) + dda3*(Izz3 + l3^2*m3 + L1*l3*m3*cos(a2 + a3) + L2*l3*m3*cos(a3)) - da2*(L1*(da2 + A1*s)*(l2*m2*sin(a2) + l3*m3*sin(a2 + a3) + L2*m3*sin(a2)) + da3*l3*m3*(L1*sin(a2 + a3) + L2*sin(a3))) - A1*s*(L1*da2*(l2*m2*sin(a2) + l3*m3*sin(a2 + a3) + L2*m3*sin(a2)) + da3*l3*m3*(L1*sin(a2 + a3) + L2*sin(a3))) + A1*s^2*(Izz1 + Izz2 + Izz3 + L1^2*m2 + L1^2*m3 + L2^2*m3 + l1^2*m1 + l2^2*m2 + l3^2*m3 + 2*L1*l3*m3*cos(a2 + a3) + 2*L1*L2*m3*cos(a2) + 2*L1*l2*m2*cos(a2) + 2*L2*l3*m3*cos(a3)) + (A1*g*m3*(L1*s - l3*sin(a2 + a3) - L2*sin(a2) + l3*s*cos(a2 + a3) + L2*s*cos(a2)))/(s^2 + 1) + (A1*g*m2*(L1*s - l2*sin(a2) + l2*s*cos(a2)))/(s^2 + 1) - da3*l3*m3*(L1*sin(a2 + a3) + L2*sin(a3))*(da2 + da3 + A1*s) + (A1*g*l1*m1*s)/(s^2 + 1)`
T2	`dda1*(Izz2 + Izz3 + m3*(L2^2 + l3^2 + 2*L2*l3*cos(a3) + (A2*L1*L2*s)/(s^2 + 1) - (A2*L1*l3*(sin(a3) - s*cos(a3)))/(s^2 + 1)) + l2*m2*(l2 + (A2*L1*s)/(s^2 + 1))) + da1*(L1*da1*((A2*l2*m2)/(s^2 + 1) + (A2*L2*m3)/(s^2 + 1) - (A2*l3*m3*(cos(a3) - s*sin(a3)))/(s^2 + 1)) - L2*da3*l3*m3*sin(a3)) + dda3*(Izz3 + l3*m3*(l3 + L2*cos(a3))) + A2*s^2*(Izz2 + Izz3 + m3*(L2^2 + 2*cos(a3)*L2*l3 + l3^2) + l2^2*m2) - g*m3*((A2*L2*(sin(a1) - s*cos(a1)))/(s^2 + 1) + (A2*l3*(sin(a1 + a3) - s*cos(a1 + a3)))/(s^2 + 1)) - (A2*g*l2*m2*(sin(a1) - s*cos(a1)))/(s^2 + 1) - L2*da3*l3*m3*sin(a3)*(da1 + da3 + A2*s) - A2*L2*da3*l3*m3*s*sin(a3)`
T3	`dda2*(Izz3 + l3*m3*(l3 + (A3*L2*s)/(s^2 + 1))) + da1*(da1*l3*m3*((A3*L2)/(s^2 + 1) - (A3*L1*(cos(a2) - s*sin(a2)))/(s^2 + 1)) + (A3*L2*da2*l3*m3)/(s^2 + 1)) + dda1*(Izz3 + l3*m3*(l3 - (A3*L1*(sin(a2) - s*cos(a2)))/(s^2 + 1) + (A3*L2*s)/(s^2 + 1))) + A3*s^2*(m3*l3^2 + Izz3) - (A3*g*l3*m3*(sin(a1 + a2) - s*cos(a1 + a2)))/(s^2 + 1) + (A3*L2*da2*l3*m3*(da1 + da2))/(s^2 + 1)`

11.3.5 Transfer Function

Given the solution found in Table 5: Laplace EOM, we may rearrange the equations found so the solution is given in terms of the transfer function $\left(TF = \frac{\theta_i}{\tau_i}\right)$. The transfer functions for the system may be found in

$\dfrac{\theta_1}{\tau_1}$	`-1/(((da2*(L1*da2*(l2*m2*sin(a2) + l3*m3*sin(a2 + a3) + L2*m3*sin(a2)) + da3*l3*m3*(L1*sin(a2 + a3) + L2*sin(a3))) - dda2*(m3*L2^2 + 2*m3*cos(a3)*L2*l3 + L1*m3*cos(a2)*L2 + m2*l2^2 + L1*m2*cos(a2)*l2 + m3*l3^2 + L1*m3*cos(a2 + a3)*l3 + Izz2 + Izz3) - dda3*(Izz3 + l3^2*m3 + L1*l3*m3*cos(a2 + a3) + L2*l3*m3*cos(a3)) + da3*l3*m3*(L1*sin(a2 + a3) + L2*sin(a3))*(da2 + da3))/(s^2*(Izz1 + Izz2 + Izz3 + L1^2*m2 + L1^2*m3 + L2^2*m3 + l1^2*m1 + l2^2*m2 + l3^2*m3 + 2*L1*l3*m3*cos(a2 + a3) + 2*L1*L2*m3*cos(a2) + 2*L1*l2*m2*cos(a2) + 2*L2*l3*m3*cos(a3)) - s*(L1*da2*(l2*m2*sin(a2) + l3*m3*sin(a2 + a3) + L2*m3*sin(a2)) + da3*l3*m3*(L1*sin(a2 + a3) + L2*sin(a3))) - L1*da2*s*(l2*m2*sin(a2) + l3*m3*sin(a2 + a3) + L2*m3*sin(a2)) + (g*m3*(L1*s - l3*sin(a2 + a3) - L2*sin(a2) + l3*s*cos(a2 + a3) + L2*s*cos(a2)))/(s^2 + 1) + (g*m2*(L1*s - l2*sin(a2) + l2*s*cos(a2)))/(s^2 + 1) - da3*l3*m3*s*(L1*sin(a2 + a3) + L2*sin(a3)) + (g*l1*m1*s)/(s^2 + 1)) - 1)*(s^2*(Izz1 + Izz2 + Izz3 + L1^2*m2 + L1^2*m3 + L2^2*m3 + l1^2*m1 + l2^2*m2 + l3^2*m3 + 2*L1*l3*m3*cos(a2 + a3) + 2*L1*L2*m3*cos(a2) + 2*L1*l2*m2*cos(a2) + 2*L2*l3*m3*cos(a3)) - s*(L1*da2*(l2*m2*sin(a2) + l3*m3*sin(a2 + a3) + L2*m3*sin(a2)) + da3*l3*m3*(L1*sin(a2 + a3) + L2*sin(a3))) - L1*da2*s*(l2*m2*sin(a2) + l3*m3*sin(a2 + a3) + L2*m3*sin(a2)) + (g*m3*(L1*s - l3*sin(a2 + a3) - L2*sin(a2) + l3*s*cos(a2 + a3) + L2*s*cos(a2)))/(s^2 + 1) + (g*m2*(L1*s - l2*sin(a2) + l2*s*cos(a2)))/(s^2 + 1) - da3*l3*m3*s*(L1*sin(a2 + a3) + L2*sin(a3)) + (g*l1*m1*s)/(s^2 + 1)))`
$\dfrac{\theta_2}{\tau_2}$	`1/(((dda1*(Izz2 + Izz3 + m3*(L2^2 + 2*cos(a3)*L2*l3 + l3^2) + l2^2*m2) + dda3*(Izz3 + l3*m3*(l3 + L2*cos(a3))) - L2*da1*da3*l3*m3*sin(a3) - L2*da3*l3*m3*sin(a3)*(da1 + da3))/(dda1*(m3*((L1*l3*(sin(a3) - s*cos(a3)))/(s^2 + 1) - (L1*L2*s)/(s^2 + 1)) - (L1*l2*m2*s)/(s^2 + 1)) - s^2*(Izz2 + Izz3 + m3*(L2^2 + 2*cos(a3)*L2*l3 + l3^2) + l2^2*m2) + g*m3*((L2*(sin(a1) - s*cos(a1)))/(s^2 + 1) + (l3*(sin(a1 + a3) - s*cos(a1 + a3)))/(s^2 + 1)) - L1*da1^2*((L2*m3)/(s^2 + 1) + (l2*m2)/(s^2 + 1) - (l3*m3*(cos(a3) - s*sin(a3)))/(s^2 + 1)) + (g*l2*m2*(sin(a1) - s*cos(a1)))/(s^2 + 1) + 2*L2*da3*l3*m3*s*sin(a3)) - 1)*(dda1*(m3*((L1*l3*(sin(a3) - s*cos(a3)))/(s^2 + 1) - (L1*L2*s)/(s^2 + 1)) - (L1*l2*m2*s)/(s^2 + 1)) - s^2*(Izz2 + Izz3 + m3*(L2^2 + 2*cos(a3)*L2*l3 + l3^2) + l2^2*m2) + g*m3*((L2*(sin(a1) - s*cos(a1)))/(s^2 + 1) + (l3*(sin(a1 + a3) - s*cos(a1 + a3)))/(s^2 + 1)) - L1*da1^2*((L2*m3)/(s^2 + 1) + (l2*m2)/(s^2 + 1) - (l3*m3*(cos(a3) - s*sin(a3)))/(s^2 + 1)) + (g*l2*m2*(sin(a1) - s*cos(a1)))/(s^2 + 1) + 2*L2*da3*l3*m3*s*sin(a3)))`
$\dfrac{\theta_3}{\tau_3}$	`1/(((dda1*(m3*l3^2 + Izz3) + dda2*(m3*l3^2 + Izz3))/(s^2*(m3*l3^2 + Izz3) + da1*(da1*l3*m3*(L2/(s^2 + 1) -`

58

```
(L1*(cos(a2) - s*sin(a2)))/(s^2 + 1)) + (L2*da2*l3*m3)/(s^2 +
1)) - dda1*l3*m3*((L1*(sin(a2) - s*cos(a2)))/(s^2 + 1) -
(L2*s)/(s^2 + 1)) - (g*l3*m3*(sin(a1 + a2) - s*cos(a1 +
a2)))/(s^2 + 1) + (L2*da2*l3*m3*(da1 + da2))/(s^2 + 1) +
(L2*dda2*l3*m3*s)/(s^2 + 1)) + 1)*(s^2*(m3*l3^2 + Izz3) +
da1*(da1*l3*m3*(L2/(s^2 + 1) - (L1*(cos(a2) - s*sin(a2)))/(s^2
+ 1)) + (L2*da2*l3*m3)/(s^2 + 1)) - dda1*l3*m3*((L1*(sin(a2) -
s*cos(a2)))/(s^2 + 1) - (L2*s)/(s^2 + 1)) - (g*l3*m3*(sin(a1 +
a2) - s*cos(a1 + a2)))/(s^2 + 1) + (L2*da2*l3*m3*(da1 +
da2))/(s^2 + 1) + (L2*dda2*l3*m3*s)/(s^2 + 1)))
```

11.3.6 PID Development

At this point we in many ways reach the limits of symbolic variables in MATLAB. PIDs can be created with tuneable parameters, so it is possible to treat the system's variables (mass, length, etc…) as tuneable values preserving our purely algebraic solution. However, this would exist as a purely intellectual exercise of no practical merit. Instead it is more prudent to develop the software to find the PID parameters for the system once basic fundamentals regarding the system can be confirmed.

See (imma_real_boy) kt for MATLAB code which shall substitute all systems variables for their actual variables (when confirmed). This shall allow the reader to solve for the "actual" PID values for their system[2].

At one point this section was to be used to show the process by which one could create the PID parameters to control the system:

- A general solution sis provided to the EOM for a 3 DOF manipulator (just sub in the desired values for p, doesn't even need to be RRR);
- The laplace transform is performed on these values; and,
- A transfer function is created from these equations.

It is trivial from this point to plug the transfer functions into MATLAB's pidTuner and generate a PID. But that's the point, its trivial, it merely shows the author is capable of using a MATLAB suite. It does not provide actual values for control (these cannot be found until there is an exoskeleton to control), and the documentation for pidTuner is sufficient that if you got this far you'll be fine.

11.3.7 PID Tuning

Why did we used PID for 1 DOF

What method did we use.

---

[2] Angles should be entered as tuneable parameters, this can then be used to find the variation in PID parameters for the full range of movement. My own analysis has found the variation sufficiently small for the range of human leg movement that PID parameters may be approximated as constant. This would allow for the creation of three independent SISO PID loops, opposed to a MIMO system.

What values were used.

Why do they look incorrect

5000

500

0

For the reasons discussed in kt to control the equipment used in the demonstration rig (a 1 DOF exoskeleton) PID control was selected.

11.4   Results and Discussion

12 Subsystem Four: Communications

This section details the analysis, design, implementation, and results of the subsystem responsible for communication between the actuation systems and the controls/perception systems.

12.1 Requirements and Functional Decomposition

The overarching purpose of subsystem four (SS4) is to communicate the desired action to the actuation system.
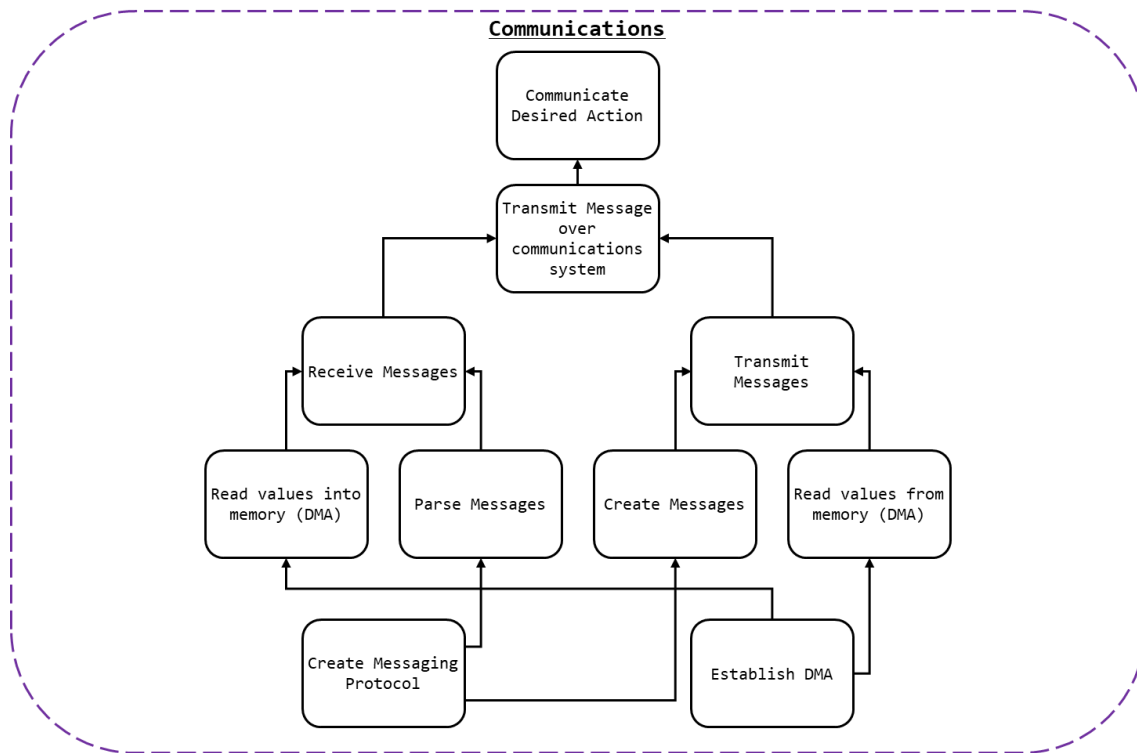
Figure 40: SS4 Breakdown

As detailed in Figure 40: SS4 Breakdown, to communicate the desired action to the actuation system:

- Messages would need to be received; and,
    - This process would involve receiving the messages; and,
    - Parsing them into useable data.
- Messages would need to be sent.
    - This process should involve creating messages; and,
    - Transmitting them.

To ensure that messages where properly interpreted and created by all parties a communication protocol and packet protocol would be need.

To store messages, received or sent, numerous methods were considered and tested. Ultimately, Direct Memory Access (DMA) was used which required that the DMA on the selected microcontroller be enabled.

12.1.1 Communication Protocol

The requirements of the communication protocol where as follows:

- ASCII messages must be transmittable;
- Synchronisation or dependency between systems is to be avoided;
- Systems which required addresses for communication were to be excluded.

12.1.2 Packet Protocol

The requirements of the packet protocol where as follows:

- Generic data types must be transmittable;
- Signed values (plus/minus) of either integers or real numbers would be sent; and,
- Start and stop bits characters would be used to indicate the beginning and the end of messages (in the case of incomplete messages, the message should be invalid).

12.1.3 Connection Method

The requirements of the connection where as follows:

- Wired connection method;
- A common ground should be established (where relevant); and,
- Where possible standardised jacks/sockets should be used.

12.2 Background and Prior Art

Parallel communication is the method of communicating a multibit message over multiple channels. With enough channels, parallel communication may be used to communicate a message of *any* size in a single clock cycle. However, communication channels can be resource intensive (i.e. using lots of cables and pins, the physical size of the interconnect).

Instead serial communication involves sending data over a single channel sequentially. While often slower than parallel communication, serial communication is often preferable due to the scarcity of I/O lines on microcontrollers. A protocol of encoding messages is used to transmit messages in a consistent intelligible manner.

Serial communication may be synchronous or asynchronous. Synchronous uses a clock signal to synchronise communication. This can result in faster more reliable communication but depends on a centralised clock signal; to maximise demarcation between the project sections, synchronous communication shall not be used.

Asynchronous serial communication may be accomplished by the use of a pair of wires (one for transmission, one for receiving) and by transmitting messages in binary. Messages which can be encoded in binary (e.g. ASCII) may be transmitted in this manner.

A universal asynchronous receiver-transmitter (UART) is a hardware device for asynchronous serial communication that may be integrated into a microcontroller.

UART may be used to implement asynchronous serial communication on a microcontroller via I/O lines.

Direct memory access (DMA) is a mechanism by which hardware systems (like UART) are able, independent of the central processing unit (CPU), to interface directly with the main system memory. By bypassing the CPU read and write operations can be completed faster, while the CPU is dedicated to other tasks. For example, messages received via UART may be directly stored in memory, and messages to be sent via UART may be loaded into buffers directly.

12.3 Approach and Execution

12.3.1 Communication Protocol

For details relating to the microcontroller selection see section (kt). As noted in section kt, two communication channels were required per microcontroller.

Two UART channels where implemented in C for the STM32 Nucleo boards. The pin used by each channel is shown in Table 7: UART Pins.

Table 7: UART Pins

UART	Function	STM32F303k8 Pin	Nucleo Connector Pin	DMA Channel
UART 1	RX	Port A Pin 10	D0	5
	TX	Port A Pin 9	D1	4
UART 2	RX	Port A Pin 3	A2	7
	TX	Port A Pin 2	A7	6

Much of the peripheral initilisation was completed used STM32CubeMX. The configuration file used can be found in kt. The configuration of both UART channels may be found in Table 8: UART Configuration.

Table 8: UART Configuration

Parameter	Value
Baud Rate	9600 Bits/s
Word Length	8 Bits (Including Parity)
Parity	None
Stop Bits	1
Alternate Function (for GPIO)	7

Each UART was configured to use DMA to receive and transmit messages. The DMA settings can be found in Table 9: DMA Configuration.

Table 9: DMA Configuration

Parameter	Value
DMA Mode	Normal (Not circular)
Data Width (Peripheral)	Byte
Data Width (Memory)	Byte

Increment Address	Memory
Priority	Medium

The process of transmitting a message was as follows:

- Ensure UART 1 and 2 were ready for transmission;
  - Via isTransmitting, which may be found in /Src/main.c
- Load message into buffer; and,
- Direct UART to transmit buffer via DMA.
  - Via HAL_UART_Transmit_DMA, which may be found in /Drivers/STM32F3xx_HAL_Driver/Src/stm32f3xx_hal_uart.c

12.3.2 Packet Protocol

As seen in Figure 41: Packet Protocol, a packet protocol was established to ensure that messages could be understood.
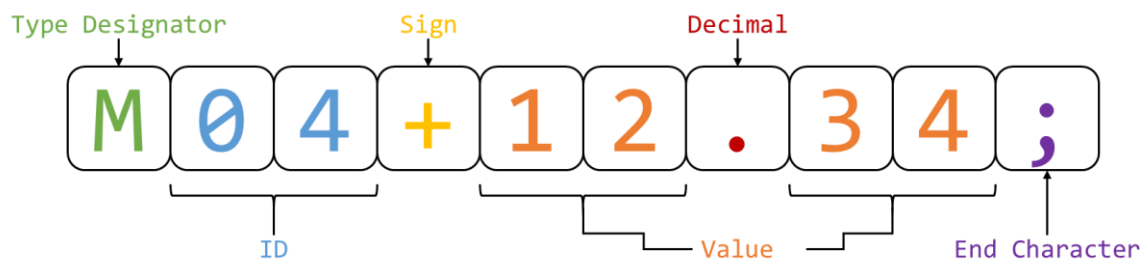

Figure 41: Packet Protocol

The protocol is detailed in Table 10: Packet Protocol:

Table 10: Packet Protocol

Value	Notes
Type Designator	The non-case-sensitive type designator indicated what type of value was being transmitted. For example, 'T' (or 't') indicated that the value represented the desired torque of an actuator. Size: 1 char
ID	The integer representing which value of a given type was being updated. For example, an ID of 03 referred to the right foot. Size: 2 chars
Sign	Used to indicate if the value was positive or negative. Size: 1 char
Value	The value being updated. This could be of any length. A left-hand side and right-hand side value (even if 0) was required for a valid message (e.g. 11 or .5 was invalid, but 11.0 and 0.5 was valid.
Decimal	Used to punctuate the value received. Indicated the end of the left-hand side of the value. Size: 1 char
End Character	Used to indicate the end of a message. Upon reading a valid message this value would be changed to an '@' to prevent the same message (within the DMA buffer) from being ready twice. Size: 1 char

This protocol was used for all communicates to, from, and within the controls/perception system.

12.3.3 Connection Method

As UART was to be used over a two-wire connection three wires in total were required:

- RX;
- TX; and,
- Ground.

A common ground ensures that all RX an TX messages where read correctly and had the same reference voltage. While numerous cable options where viable, Category 5 cable, or CAT 5, cables where selected to connect devices together.

CAT 5 cables are twisted pair cables (4 sets) commonly used in ethernet connection. CAT 5 cable were terminated with 8P8C modular connectors and plugged into female RJ45 connectors. As CAT 5 cables feature more than three wires it became possible to provide 5V across boards, this is discussed in further detail in kt. These connectors were then mounted on the controller PCB, see kt.

12.4 Results and Discussion

SS4 was tested by daisy chaining multiple controller boards together via 1.5m CAT 5e cables. Each board would transmit the messages relevant to it on both UART 1 and UART 2. Messages received would be parse. Invalid messages were discarded. Valid messages where then passed along the chain to ensure all controller boards were informed, e.g. valid messages incoming to UART 1 were sent outgoing to UART 2.

For the thesis demonstration, two boards where connected and sensor readings from one board were used to communicate actuator commands to the other.

In both these test case the communication system was perfectly functioning. Messages were sent and transfer, no corrupt messages were interpreted as valid, and messages where interpreted correctly.

The interface between the actuation system and the controls/perception system was never completed. Provisions were made for connection to another system (these were also used for debugging), see kt, but were tested as the actuation system was never completed. While one can be confident that the communication system would function as required, it cannot be said for certain without testing.

12.4.1 Communication speed

It is difficult to say if the communication system would have been fast enough to allow for real time control of the system. While messages were kept short and DMA was employed to speed messaging the baud rate of 9600 may have been simply too low for the communication speeds required.

Given an 8-bit char (ASCII character) approximately 109 messages (of standard size) could be sent per second, or about 9ms per message. Given the potential for a message to be passed on up to 6 times before being interpreted by the actuation system, and that up to 5 messages may be queued to be sent by each controller, a maximum delay of 192ms (21 message periods) could be expected. Given a human reaction time of $150 - 300$ms (Yuhas, 2012), a system with a reaction time of 192ms will lag behind the user and not react sufficiently quickly.

Going forward it is recommended that the baud rate of the system is raised to 115200 bits/s. Transmitting messages twelve times faster will result in a reaction time of 16ms and reduce the possibility of lag.

13 Subsystem Five: Actuation Systems

This section details the analysis, design, implementation, and results of the subsystem responsible for interfacing and actuating actuators to demonstrate the functionality of the other major subsystems.

13.1 Requirements and Functional Decomposition

The overarching purpose of subsystem five (SS5), in lieu of the final exoskeleton actuator system, is to demonstrate the functionality of the other subsystems (and the project in general).
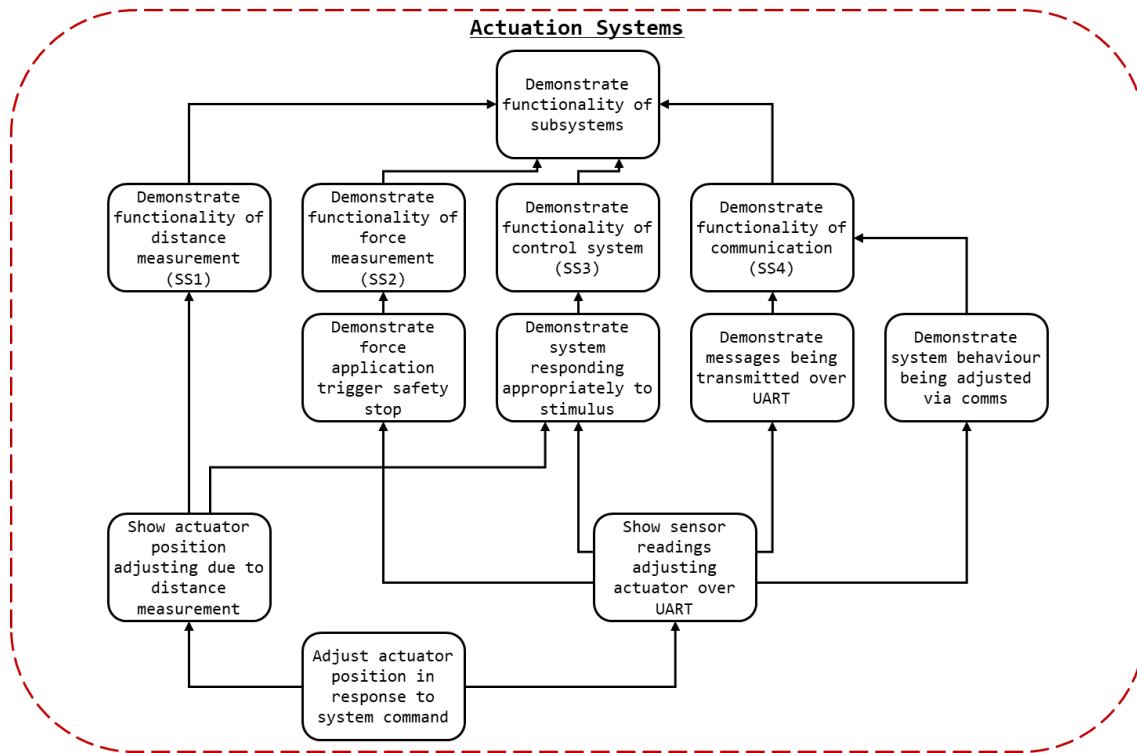

Figure 42: SS5 Breakdown

As detailed in Figure 42: SS5 Breakdown to demonstrate the functionality of the other major subsystems two representative action sets can be completed. The functionality of SS2,3, and 4 can be demonstrated by showing that force sensors readings from one device can, over the communication system, can shut off the operation of an actuator when the external force exceeds the internal force. The functionality of SS1 and 3 can be shown by demonstrating that the position of an actuator can be controlled by position sensor readings.

The functionality of both these tests however, is dependent on the behaviour of an actuator as directed by the system. The reason for two tests, rather than a single integrated test was a consequence of servomotor lead time, as noted in kt.

13.2 Background and Prior Art

13.2.1 Servomotor

A servomotor is a linear or rotary actuator with a closed-loop control system used to manage its behaviour. Usually a motor will be paired with an encoder to provide feedback to the system. The specific of the implementation of servomotors vary, as does their ability to control position, velocity, and acceleration.

13.2.2 Pulse Width Modulation (PWM)

Pulse-width modulation (PWM) is a modulation technique most commonly used to encode and control the power output of motors. PWM works by toggling the output signal to a load sufficiently quickly to approximate analogue behaviour. I.e. in a system where power cannot directly be controlled, PWM can be used to ensure that the output signal is high 50% of the time, effectively demanding 50% power to be supplied. As long as the switching frequency is so high as for the resultant waveform to be perceived as continuous the load will behave as if driven by a continuous supply.

For the control of servomotors PWM is often used to indicate the desired behaviour (indicating position, speed, etc…). The signal delivered to the servomotor will be held low and then toggled high for a duration. The duration of the high period, or pulse, in relation to a full cycle period is the duty cycle. The duty cycle indicates to the servo the desired behaviour, see kt.

13.3 Approach and Execution

13.3.1 Actuators

Due to the time constraints associated with creating SS5 and the goal of demonstrating SS1-4 (not creating a functional exoskeleton), rather than creating a servomotor a prefabricated servomotor was selected as the desired actuator for SS5.

As the lead time associated with most high precision servomotors was beyond the remainder of the project when SS5 was commissioned (in response to learning there would be no exoskeleton) the selection of servomotors available to the project was limited. As such, there were no servomotors available capable of actuating with the force sensor plate attached (the torque requirements were simply too high).

For demonstrating the efficacy of the position system, the strongest servomotor available (by torque) was selected. Greater torque would allow for greater control authority when accelerating, and as the mock exoskeleton (see kt) would be constructed from suboptimal materials greater control authority was a priority. Thus, the MG995 servomotor was selected, see figure kt.

Figure 43: MG995 - High Speed Metal Gear Dual Ball Bearing Servo

The MG995 datasheet may be found in the attached documents as "MG995 - High Speed Metal Gear Dual Ball Bearing Servo.pdf". The MG995 offered position-based control and 0.98 Nm (10 kgf cm) of torque (at 6V).

For demonstrating the efficacy of the force detection systems a continuous rotation servo was selected as it could stop when the external force on the suit exceeded the force internal, and could vary its speed depending on the force applied internally. Due to its availability the 900-00008 Continuous Rotation Servomotor was selected.

Figure 44: 900-00008 - Continuous Rotation Servo

The 900-00008 datasheet may be found in the attached documents as "900-00008 - Continuous Rotation Servo.pdf".

To power and control the servomotors a PWM generated by the nucleo boards was used. As the PCBs designed, see kt, did not consider SS5 within scope at the time of fabrication, there were no dedicated headers for powering the servo. Later iterations remedied this by adding a dedicated servo header. For creating the configurations discussed in SS5 fly-wires were solder to the board, and the connections were heat shrunk, see kt. While this is suboptimal, it did allow for reliable and consistent control of the servomotors.

13.3.2 Test A: Position detection

The first test, to demonstrate SS1 and SS3, would entail attaching the position detection system to a rod at the end of a servomotor and controlling the motor/rod position based on the position readings. Effectively a two-limb-segments/one-joint mock exoskeleton.

As seen in Figure 45: Test A Configuration, A fixed exoskeleton segment (A) is installed flush with a pilot limb segment (B) (e.g. thigh, bicep). At the joint and actuator (S) is used to rotate a free exoskeleton segment (C) flush and parallel to a limb segment of the pilot (D) (e.g. shin, forearm). The IR sensor frame (E) is mounted to the end of C and IR sensors (F) may determine the position of D.
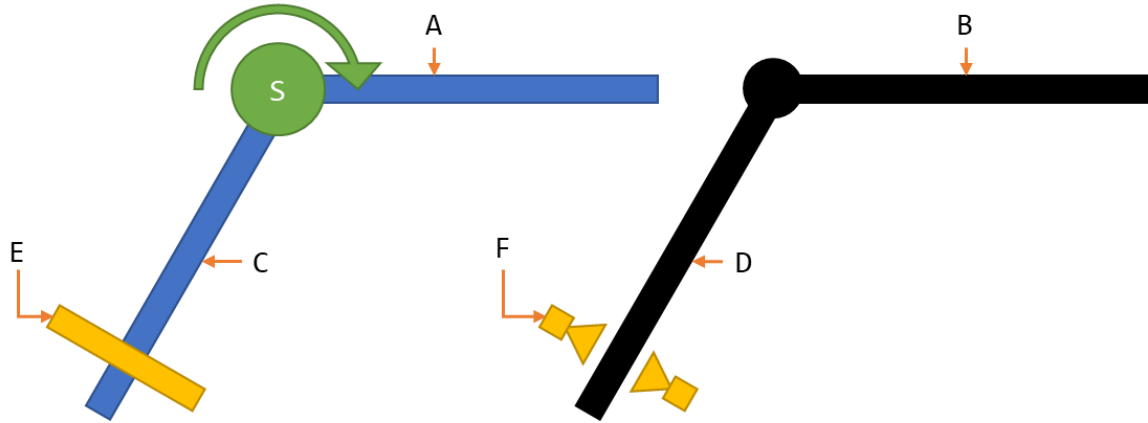

Figure 45: Test A Configuration

The MG995, discussed in kt, was used as the actuator for Test A. Aluminium beams (x mm) kt were used for the exoskeleton segments. To minimise the weight of the perception system, the power supply for the servo, SS1, and SS3 where located on the upper segment. Additionally, the controls board was also located on the upper segment.

To mount the lower segment to the servomotor, cable ties were used to attach the segment to a servo horn. A bolt hole placed in the segment was then used to screw the servo horn, servomotor, and segment together, see kt.

13.3.3 Test B: Force detection
The second test, to demonstrate SS2, SS3, and SS4, would entail connecting two boards via CAT 5e cables. As seen in Figure 46: Test B Configuration, one board (B) would send force measurements from SS2 (A) over the SS4 (C) and the other (D) would control an actuator (S) based on the received values.
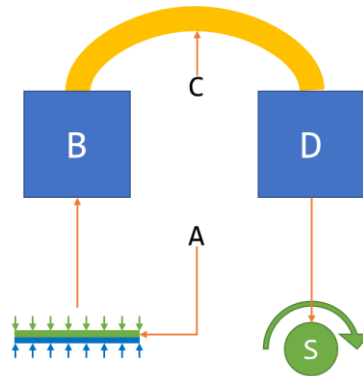

Figure 46: Test B Configuration

70

A single short aluminium beam (x mm) kt was used as a platform for the test. Both boards were mounted to the beam. A CAT 5e cable was used to connect the two boards together.

13.3.4 PWM Control

To control the servomotors PWM control was required.

For details relating to the microcontroller selection see section (kt).

A single PWM output channel was implemented in C for the STM32 Nucleo boards. Much of the peripheral initialisation was completed used STM32CubeMX. The configuration file used can be found in kt. The configuration of the PWM, including GPIO used, can be found in Table 11: PWM Configuration.

Table 11: PWM Configuration

Parameter	Value
STM32F303k8 Pin	Port B Pin 4
Nucleo Connector Pin	D12
Timer	3
Channel	1
Prescaler (PSC - 16 bits value)	72
Counter Mode	Up
Counter Period (AutoReload Register - 16 bits value)	100
Internal Clock Division (CKD)	No Division
Auto-reload preload	Disabled
PWM Generation Channel 1 Mode	PWM Mode 1

Once the PWM was initialised, the following methods was required for control:

- Start the PWM (HAL_TIM_PWM_Start(&htim3, TIM_CHANNEL_1))
- Determine Duty Cycle (volatile int DC;)
- Updated desired pulse width (set_pulse_width(void))
- Set the new pulse width & duty cycle, (__HAL_TIM_SET_COMPARE(&htim3, TIM_CHANNEL_1, pulse_width);

This could be used to control behaviour of the motors given the configuration, see Table 12: Motor PWM Requirements.

Table 12: Motor PWM Requirements

Test A (MG995)	
Cycle Period	20 ms (50 Hz)
Min Pulse (-60 Deg)	0.7 ms
Max Pulse (+60 Deg)	2.5 ms
Idle Pulse (0 Deg)	1.5 ms
Test B (900-00008)	
Cycle Period	20 ms (50 Hz)

Min Pulse (-50 rpm)	1.3 ms
Max Pulse (+50 rpm)	1.7 ms
Idle Pulse (0 rpm)	1.5 ms

13.4 Results and Discussion

This section will detail the performance of the actuators selected and their interface with the supersystems. For discussion relating to the systems performance in Test A and Test B see section kt.

To summarise the results of SS5, it works but its ugly. We begin with the ugly.

The attachment mechanism for mounting associated with the servomotors depended on cable ties. While cable ties are perfectly adequate for cable management, and function well as a stand in for hose clamps at small diameters, they are not a robust or rigid method of fasting motors in place. In further iterations of the system it is strongly recommended that dedicated mounts for the servomotors be commissioned.

The exoskeleton segments, comprised of aluminium, were heavy and flexible. In Test A, a finger's touch could cause the lower exoskeleton segment to wobble and flex. The system when tested would oscillate if accelerated too quickly, confusing the perception systems. This effectively capped the accuracy of the perception system and the speeds (and response times) at which stability could be attained.

Motor selection should not be determined by lead time. Instead actuators should be selected based their requirements. Originally the 900-00008 was to be used for Test A, but upon preliminary testing it was found that it lacked the torque to lift the lower exoskeleton segment beyond 30 degrees.

Neither servomotor allowed for control via torque or acceleration, the control variable used in SS3. Instead position and velocity were controlled. However, they could not be measured so the acceleration could not be indirectly controlled. The servomotors had their own internal control mechanisms, which had to be compensated for. Finally, the resolution of the MG995 was so low as to be visually perceptible. For all further iteration of the system it is strongly suggested that the actuators be reengineered.

Soldering loose cables to the through holes of a PCB header to control a system's actuators is… not best practice. While later iterations of the PCB included dedicate servo headers, the PCBs used for demonstration featured fly-wires.

The battery system used for SS5 was functional but ramshackle. An 8-battery receptacle was modified to fit 4 batteries to power the 6V MG995. This should be replaced with a 4-battery receptacle.

Preferential to the improvements discussed SS5 should be make redundant. *A functioning actuation and structural system would eliminate the need for SS5 entirely.*

Areas of possible improvement considered, SS5 as a whole worked, and performed as desired.

Analysis via logic analyser indicated that the PWM generation worked correctly in all circumstances. The PWM implemented worked correctly in all circumstances it was tested. The code developed was effective and functional.

The motors when testing in isolation or in Test A and Test B performed as instructed. While the response time of the MG995 was slower than preferred, it was adequate to demonstrate the functionality of perception systems.

14 Integrated Exoskeleton

This system details the process of integrating the engineered solutions of the major subsections of the project. Then the final holistic system commissioned is detailed.

14.1 Requirements and Functional Decomposition

14.2 Prior Art

14.3 Solution

14.4 Implementation

A "Signal, Voltage High, Ground" standardisation was placed on all inputs and ouputs as best practice for the entire project.

3.3 holes, 3.5mm drill bit, M3 screws

Powering devices via ethernet

14.5 Results

15 Results and Performance

16 Recommendations and Further Works

16.1 SS1

- Use hose clamps

16.2 SS2

16.3 SS3

16.4 SS4

16.5 SS5

16.6 Exoskeleton

17 Conclusion

18 Bibliography

Agarwal, A. (2005). *Foundations of analog & digital electronic circuits* (1 ed.). Massachusetts: Massachusetts Institute of Technology. Retrieved June 1, 2018, from https://www.google.com/url?sa=t&rct=j&q=&esrc=s&source=web&cd=1&ved=0ahUKEwiBu7yQl7LbAhUEoZQKHfYlBzkQFggpMAA&url=http%3A%2F%2Fsiva.bgk.uni-obuda.hu%2Fjegyzetek%2FMechatronikai_alapismeretek%2FEnglish_Mechatr%2FElectr_Eng-1%2FLiterature%2FFoundations%2520o

American Technologies Network Corporation. (2018, May 30). *How Does Night Vision Work.* Retrieved from atncorp.com: https://www.atncorp.com/hownightvisionworks

Arrow. (2018). *Magnetoresistive Sensor.* Retrieved May 30, 2018, from arrow.com: https://www.arrow.com/en/categories/sensors/magnetoresistive-sensors

Axe, D. (2012, May 23). *Combat Exoskeleton Marches Toward Afghanistan Deployment.* Retrieved May 30, 2018, from Wired: https://www.wired.com/2012/05/combat-exoskeleton-afghanistan/

Bulgrin, M. (2017, May 11). *The History of the Hose Clamp.* Retrieved from normagroup.com: https://blog.normagroup.com/en/the-history-of-the-hose-clamp/

Bunnings. (2018, May 31). *Kinetic 21 - 44mm 304 Stainless Steel Hose Clamp.* Retrieved May 31, 2018, from Bunnings.com: https://www.bunnings.com.au/kinetic-21-44mm-304-stainless-steel-hose-clamp_p4920194

Charara, S. (2015, July 9). *This robotic exoskeleton helps paralysed patients to walk and it's getting smarter.* Retrieved August 23, 2017, from Wearable: https://www.wareable.com/wearable-tech/exoskeleton-paralysed-patients-ekso-bionics-gt-sarah-thomas

Computer Cable Store. (2018, May 31). *11 7/8 Inch Black Standard Nylon Cable Tie - 100 Pack.* Retrieved May 31, 2018, from computercablestore.com: https://www.computercablestore.com/11-78-inch-black-standard-nylon-cable-tie-100-pack

Cornwall, W. (2015, October 15). *Feature: Can we build an 'Iron Man' suit that gives soldiers a robotic boost?* Retrieved August 20, 2017, from sciencemag.org: http://www.sciencemag.org/news/2015/10/feature-can-we-build-iron-man-suit-gives-soldiers-robotic-boost

Cracknell, A. P., & Hayes, L. (2007). *Introduction to Remote Sensing* (2 ed.). London: Taylor and Francis. Retrieved May 30, 2018

Cutnell, J. D., & Johnson, K. W. (1998). *Physics* (4th ed.). New York: Wiley.

Cyberdyne. (2015, August 1). *CYBERDYNE Inc. has begun seeking approval from the U. S. Food and Drug Administration (FDA)*. Retrieved August 23, 2017, from cyberdyne.jp: https://www.cyberdyne.jp/english/company/PressReleases_detail.html?id=1075

Cyberdyne. (2016). *What's HAL?* Retrieved August 19, 2017, from cyberdyne.jp: https://www.cyberdyne.jp/english/products/HAL/

Cybernetic Zoo. (2010, October 14). *1890 – Assisted-walking Device – Nicholas Yagn (Russian)*. Retrieved May 30, 2018, from Cyberneticzoo.com: http://cyberneticzoo.com/tag/nicholas-yagn/

Cybernetic Zoo. (2010, April 10). *1965-71 – G.E. Hardiman I Exoskeleton – Ralph Mosher (American)*. Retrieved May 30, 2018, from cyberneticzoo.com: http://cyberneticzoo.com/man-amplifiers/1966-69-g-e-hardiman-i-ralph-mosher-american/

Dawkins, P. (2018). *Differential Equations - Notes - Laplace's Equation*. Retrieved June 3, 2018, from Paul's Online Math Notes: http://tutorial.math.lamar.edu/Classes/DE/LaplacesEqn.aspx

Dorf, R. C., & Bishop, R. H. (2011). *Modern Control Systems* (12 ed.). Upper Saddle River: Pearson.

Dunietz, J. (2017, July 27). *Robotic Exoskeleton Adapts While It's Worn*. Retrieved August 20, 2017, from scientificamerican.com: https://www.scientificamerican.com/article/robotic-exoskeleton-ldquo-evolves-rdquo-while-its-worn/

Future Electronics. (2018, May 30). *What is Optoelectronics?* Retrieved from Future Electronics: http://www.futureelectronics.com/en/optoelectronics/infrared-receivers.aspx

Garbett, I. (2001, Janurary 1). *Light attenuation and exponential laws*. Retrieved May 30, 2018, from plus.maths.org: https://plus.maths.org/content/light-attenuation-and-exponential-laws

Golnaraghi, F., & Kuo, B. C. (2010). *Automatic Control Systems* (9 ed.). Hoboken: John Wiley & Sons, Inc. Retrieved June 4, 2018

Gross, K. (2018, Feburary 19). *Ultrasonic Sensors: Advantages and Limitations*. Retrieved May 30, 2018, from MaxBotix: https://www.maxbotix.com/articles/advantages-limitations-ultrasonic-sensors.htm/

Jackson, R., Green, K. R., & Eisenbeis, R. (2017). *Achieve greater precision, reliability with integrated magnetic sensing technology*. Retrieved May 30, 2018, from ti.com:

http://www.ti.com/general/docs/lit/getliterature.tsp?baseLiteratureNumber=sszy030&fileType=pdf

Karlin, S. (2011, July 29). *Raytheon Sarcos's Exoskeleton Nears Production.* Retrieved August 11, 2017, from spectrum.ieee.org: http://spectrum.ieee.org/at-work/innovation/raytheon-sarcoss-exoskeleton-nears-produc

Keller, M. (2016, August 25). *Exoskeleton - Do You Even Lift, Bro? Hardiman Was GE's Muscular Take On The Human-Machine Interface.* (General Electric) Retrieved May 30, 2018, from GE Reports: https://www.ge.com/reports/do-you-even-lift-bro-hardiman-and-the-human-machine-interface/

Keyence Corporation. (2018). *What is a Inductive Proximity Sensor?* Retrieved May 30, 2018, from keyence.com: https://www.keyence.com/ss/products/sensor/sensorbasics/proximity/info/

Khatib, O. (2008). Chapter 5 - Dynamics. In O. Khatib, *Introduction to Robotics* (pp. 125-150). Stanford: Stanford University.

Liew, S. C. (2018, May 30). *Electromagnetic Waves.* Retrieved from Centre for Remote Imaging, Sensing and Processing.: https://crisp.nus.edu.sg/~research/tutorial/em.htm

Lynch, D. K., & Livingston, W. C. (2001). *Color and Light in Nature* (2nd ed.). Cambridge, United Kingdom: Cambridge University Press. Retrieved May 30, 2018, from https://books.google.com.au/books?id=4Abp5FdhskAC&pg=PA231&redir_esc=y#v=onepage&q&f=false

Merriam-Webster Dictionary. (2018, May 18). *noise.* Retrieved May 30, 2018, from merriam-webster.com: https://www.merriam-webster.com/dictionary/noise

National Instruments. (2018). *PID Theory Explained.* Retrieved June 4, 2018, from NationalInstruments.com: http://www.ni.com/white-paper/3782/en/

Ogata, K. (2010). *Modern Control Engineering* (2 ed.). New Jersey, United States of America: Prentice Hall. Retrieved August 25, 2017

Otaga, K. (2004). *System Dynamics* (4 ed.). Upper Saddle River: Pearson. Retrieved June 4, 2018

Robomart. (2015, November 9). *Advantages and Disadvantages of ultrasonic distance sensor.* Retrieved May 30, 2018, from Robomart: http://roboticsensors.blogspot.com/2015/11/advantages-and-disadvantages-of.html

Siciliano, B., & Khatib, O. (2016). *Springer Handbook of Robotics* (2 ed.). (B. Siciliano, & O. Khatib, Eds.) Berlin: Springer Nature. doi:10.1007/978-3-319-32552-1

Texas Instruments Incorporated. (2017). *Hall effect sensors*. Retrieved May 30, 2018, from ti.com: http://www.ti.com/sensing-products/magnetic-sensors/hall-effect/overview.html

Thomas Publishing Company. (2018). *Capacitive Proximity Sensors*. Retrieved May 30, 2018, from Thomas: https://www.thomasnet.com/articles/instruments-controls/proximity-sensors

Vishay Semiconductors. (2017, February 8). TCRT5000 - Reflective Optical Sensor with Transistor Output.

Yagin, N. (1890, February 11). *United States of America Patent No. 440684.*

Yuhas, D. (2012, May 24). *Speedy Science: How Fast Can You React?* Retrieved from scientificamerican.com: https://www.scientificamerican.com/article/bring-science-home-reaction-time/

ZJIA. (2018, June 1). *Generic YZC-161B 50kg Body Scale Sensor Human Scale Weighing Load Cell Sensor (Pack of 4)* . Retrieved June 1, 2018, from Amazon.com: https://www.amazon.com/Generic-YZC-161B-Scale-Sensor-Weighing/dp/B00MTJ6WZ2

19 Appendices

19.1 Representative Movements

19.1.1 Level One Functionality: Standing

To stand while the exoskeleton system is engaged requires the system to be capable of achieving equilibrium and control in a static environment.

Level one functionality demonstrates that for an instantaneous snapshot of operation that the system is capable of regulated operation. Note, level one functionality may also highlight the system's ability to compensate for steady state error.

19.1.2 Level Two Functionality: Squatting

Level two functionality requires level one functionality.

To squat while the exoskeleton system is engaged requires the system to be capable of control in a dynamic environment where the pilot is moving. A squat allows for the pilot to engage in motion at the stable pace of the exoskeleton, and as such may non-real-time operations.

Level two functionality demonstrates that the system is capable on a fundamental level of mirroring the pilot's movements.

19.1.3 Level Three Functionality: Stair Climbing

Level three functionality requires level two functionality.

To climb up stairs while the exoskeleton system is engaged requires the system to be capable of control in a dynamic environment where the pilot is moving while also applying force to the environment. However, should the system apply too much force to the environment the exoskeleton will simply lift itself off the ground, ultimately not requiring meaningful force regulation.

Level three functionality demonstrates that the system is capable of applying force to an environment.

19.1.4 Level Four Functionality: Sitting

Level four functionality requires level three functionality.

To sit down while the exoskeleton system is engaged requires the system to be capable of control in a dynamic environment where the pilot is moving while also applying force to the environment in a regulated manner. If the suit applied too great a force to a seat, then it may damage the seat. If the system is incapable of allowing the user to rest on the system, it may result in uncontrolled behaviour. As the pilot sits the system should concede to the force applied by the seat, until the point at which the plot applies force to the upper thighs of the system.

Simply, if a suit is capable of sitting, it is capable of interacting with the environment without destroying. Level four functionality demonstrates that the

system is capable of applying force to an environment in a safe and regulated manner.

19.1.5 Level Five Functionality: Standing/Walking/Sprinting

Level five functionality requires level four functionality.

Presuming all prior levels of functionality are attained the suit should be capable of all required actions. However, to switch contexts and move between standing, moving, and running actions requires dynamic real time control. For an exoskeleton system to be truly viable, it is essential that context switching, and real time control are possible.

Level five functionality demonstrates that the system is capable of acting in a real environment and acts as a complete proof of concept for position-based control methods.

19.2 Functional Decomposition
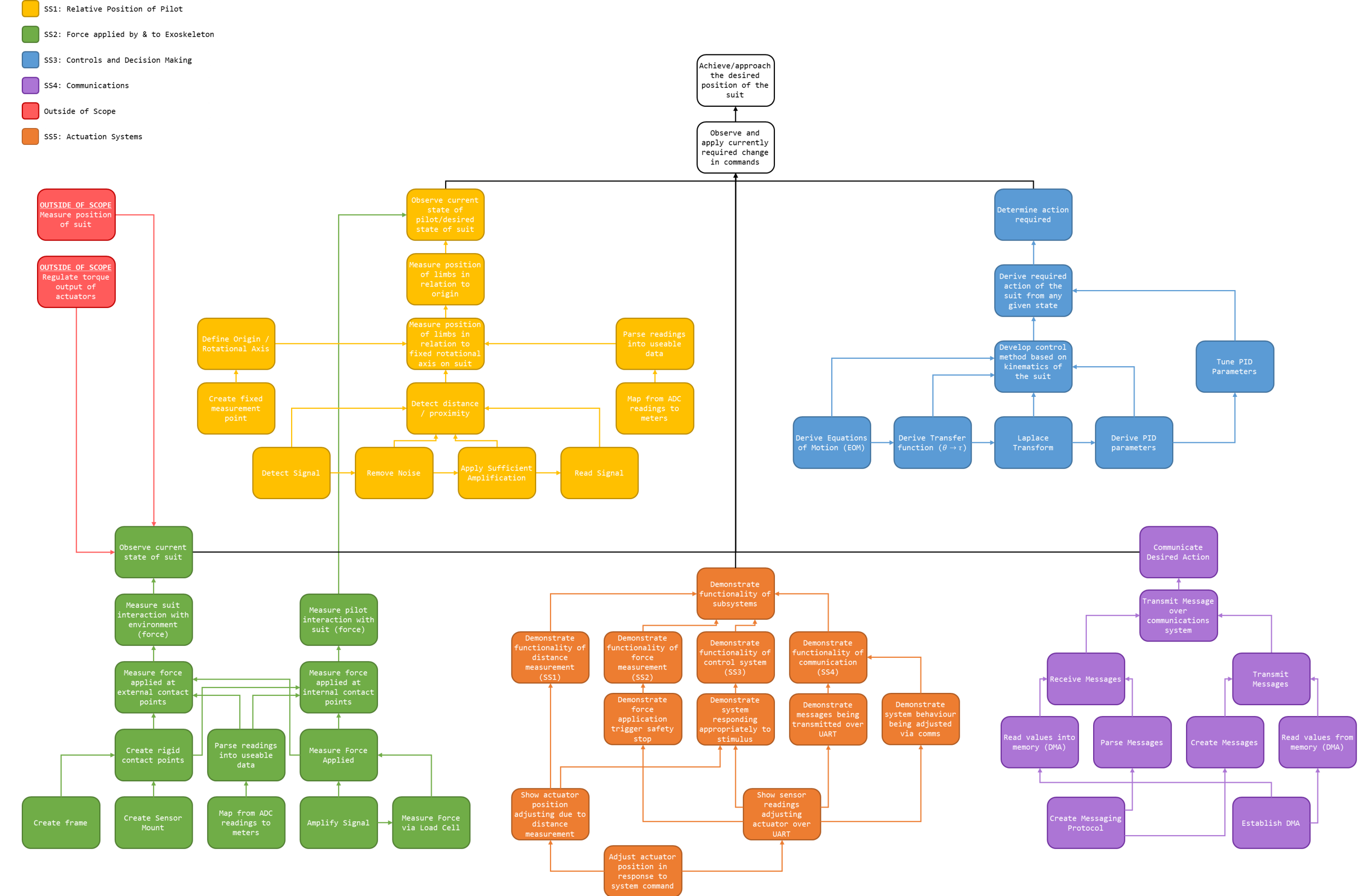
19.3 Unsuitable Proximity Sensors

19.3.1.1 Ultrasonic Range Finders

Ultrasonic waves are sound waves with a frequency above the audible range of humans, approximately 20 kHz (Cutnell & Johnson, 1998). Ultrasonic waves can used for range finding by emitting an ultrasonic sound and recording the time for the wave to be reflected back. Ultrasonic range finders have been used as the autofocus in cameras, and motion detectors, and are the underlying technology for Sonar.

Ultrasonic ranger sensors have the advantages of (Gross, 2018):

- not being dependant on the lighting conditions and offering reasonably high resolution at short distances; and,
- using sound rather than light, ultrasonic range finders are adept at detecting clear or transparent objects.

However, ultrasonic range finders have limitations (Robomart, 2015):

- they feature a minimum effective range, preventing their noncontact use at close range;
- the transmission of ultrasonic waves is affected by temperatures, humidity, and airborne particles; altering the perceived distance;
- for accurate measurement they require a hard, flat, level surface directly opposite and perpendicular. Compared to the irregular shapes and the hair of the human form, they may be ill suited; and,
- they are effect by ambient acoustic noise. The operation of the exoskeleton itself (specifically actuators) may create sufficient noise to interfere with any ultrasonic range finding.

19.3.1.2 Capacitive Proximity Sensors

Capacitive proximity sensors act in the manner of a capacitor where one plate functions as an output or a switch (Thomas Publishing Company, 2018). Capacitive proximity sensors are effective in high precision applications and controlled environments; however, they are less effective at greater ranges. Given the possibility of large uneven surfaces, comprised of unspecified materials capacitive proximity sensors were neglected from further consideration (Thomas Publishing Company, 2018).

19.3.1.3 Inductive Proximity Sensors

Inductive proximity sensors operate by the induction of eddy currents in metals and similarly conductive materials (Keyence Corporation, 2018). Humans are not metals or similarly conductive material, and as such not suitable for range finding via inductive proximity sensors (Keyence Corporation, 2018).

19.3.1.4 *Magnetic Sensors*

Range finding is possible using hall effect sensors (Texas Instruments Incorporated, 2017), magnetometers (Jackson, Green, & Eisenbeis, 2017), and Magnetoresistive Sensors (Arrow, 2018). While future iteration of the exoskeleton may include proximity detection based on magnetic sensors, they all depend on magnets (permanent or otherwise) to generate a field to be measured. In keeping the spirit of the *"Bubble"* design of the exoskeleton, it was elected to avoid perception methods that require sensors to be mounted to the pilot, and therefore, all magnetic sensors were excluded from selection.